

Dynamo Models for Planets Other Than Earth

Sabine Stanley · Gary A. Glatzmaier

Received: 6 May 2009 / Accepted: 4 August 2009 / Published online: 28 October 2009
© The Author(s) 2009

Abstract Observations from planetary spacecraft missions have demonstrated a spectrum of dynamo behaviour in planets. From currently active dynamos, to remanent crustal fields from past dynamo action, to no observed magnetization, the planets and moons in our solar system offer magnetic clues to their interior structure and evolution. Here we review numerical dynamo simulations for planets other than Earth. For the terrestrial planets and satellites, we discuss specific magnetic field oddities that dynamo models attempt to explain. For the giant planets, we discuss both non-magnetic and magnetic convection models and their ability to reproduce observations of surface zonal flows and magnetic field morphology. Future improvements to numerical models and new missions to collect planetary magnetic data will continue to improve our understanding of the magnetic field generation process inside planets.

Keywords Planetary magnetic fields · Planetary dynamos · Numerical dynamo models

PACS 91.25.Cw · 91.25.Za · 96.12.Hg · 96.12.Pc · 96.15.Gh · 96.15.Nd

1 Introduction

In the past four decades, magnetometers have flown on missions to every planet in the solar system. Magnetic field observations have demonstrated the diversity of planetary magnetic fields and provided vital information on planetary interiors. Earth, Jupiter, Saturn, Uranus, Neptune, Ganymede and most likely Mercury have active dynamos generating magnetic

S. Stanley (✉)
Department of Physics, University of Toronto, 60 St. George St., Toronto, ON, M5S1A7, Canada
e-mail: stanley@physics.utoronto.ca

G.A. Glatzmaier
Earth and Planetary Sciences Department, Earth and Marine Sciences Building,
University of California, Santa Cruz, CA 95064, USA
e-mail: glatz@es.ucsc.edu

fields. Earth, Moon, Mars, and possibly Mercury, have remanent crustal fields due to dynamo action in their ancient pasts. For more details on planetary magnetic fields, we refer the reader to papers by Hulot et al., Langlais et al., Dougherty and Russell, Jia et al., and Anderson in this issue.

Over the past two decades, numerical dynamo simulations have been used to investigate planetary magnetic fields. Although the majority of these simulations were investigations of Earth's dynamo, studies of other planetary dynamos have flourished in recent years. In this paper, we review dynamo models for planets other than Earth. We discuss the differences in planetary magnetic fields which modelers attempt to explain as well as the differences in planetary interiors which need to be included in the models. We will concentrate on the aspects of dynamo modeling that are pertinent to our objectives here. For further details on the theory and modeling of dynamos, we refer the reader to the papers by Wicht and Tilgner and by Christensen in this issue.

Numerical dynamo models discretize and evolve the equations governing magnetic field generation in an electrically conducting fluid spherical shell. The system is governed by the following equations:

- Conservation of mass:

$$\frac{D\rho}{Dt} = -\rho(\nabla \cdot \mathbf{u}) \quad (1)$$

where ρ is density, D/Dt is the Lagrangian derivative, and \mathbf{u} is velocity.

- The magnetic induction equation:

$$\frac{\partial \mathbf{B}}{\partial t} = \nabla \times (\mathbf{u} \times \mathbf{B}) - \nabla \times (\lambda \nabla \times \mathbf{B}) \quad (2)$$

where \mathbf{B} is magnetic field, and $\lambda = (\sigma \mu_0)^{-1}$ is the magnetic diffusivity where σ is electrical conductivity and μ_0 is the magnetic permeability.

- The momentum equation:

$$\rho \frac{D\mathbf{u}}{Dt} + 2\rho \boldsymbol{\Omega} \times \mathbf{u} = -\nabla P + \rho \mathbf{g} + \mathbf{J} \times \mathbf{B} + \nabla \cdot \boldsymbol{\tau} \quad (3)$$

where $\boldsymbol{\Omega}$ is the angular velocity of the rotating frame of reference, P is pressure, \mathbf{g} is the gravitational acceleration, \mathbf{J} is current density, and $\boldsymbol{\tau}$ is the deviatoric stress tensor.

- A prescribed equation of state (EOS):

$$\rho = \rho(T, P) \quad (4)$$

where T is temperature. The EOS is typically chosen to be the liquid EOS for the fluid cores of terrestrial planets and the perfect gas EOS for the atmospheres and shallow interiors of giant planets.

- The energy equation:

$$\rho C_p \frac{DT}{Dt} - \alpha_T T \frac{DP}{Dt} = \frac{J^2}{\sigma} + \boldsymbol{\tau} : \nabla \mathbf{u} + H - \nabla \cdot \mathbf{q} \quad (5)$$

where C_p is the specific heat at constant pressure, α_T is the coefficient of thermal expansion, H is the volumetric heat sources, and \mathbf{q} is heat flux.

Aside from assuming a single component fluid, we have kept the equations quite general. All planetary dynamo models solve these equations, but different approximations, boundary conditions, stability and parameter regimes may be used in simulating the different planets.

The timescales associated with fast acoustic and seismic waves in the core are not important for dynamo processes. Therefore, models usually filter out these waves by making either the Boussinesq or anelastic approximation, both of which take $\partial\rho/\partial t = 0$ in the conservation of mass equation and instead, solve for the evolution of density via (3)–(5). The Boussinesq approximation goes further by assuming a constant density except for in the buoyancy term and also assuming that density is only a weak function of temperature. The Boussinesq approximation is technically only valid for planets where the density scale height is much larger than the depth of the convective shell being considered. It is relatively acceptable for the terrestrial planets. For example, the largest terrestrial planet, Earth, has $r_o \approx 0.4H_T$ where $H_T = C_P/\alpha_T g$ is the average density scale height in the outer fluid core and r_o is the core radius.

For the giant planets, the anelastic approximation is the better approximation since the convective shell thicknesses can be much larger than the scale height. However, some giant planet dynamo models use the Boussinesq approximation as a simplification if they are interested in understanding certain mechanisms or features of the magnetic field that may not be a direct consequence of the density stratification of the fluid. The local density scale height is also a strong function of radius, being orders of magnitude larger in the deep interior than near the surface of a giant planet. Therefore, it can be argued that the Boussinesq approximation is justified in the very deep interior of a giant planet.

In the following sections, we discuss various planetary dynamo models. Section 2 deals with the two terrestrial planets other than Earth for which we have evidence of current or past dynamo action. The dynamo models for these planets are usually concerned with explaining anomalous (i.e. non-Earth-like) magnetic observations and the solutions usually appeal to some combination of core geometry, convective stability or mantle influence. Because we have no observations of time variation or core fluid flows for these terrestrial planets, the only core properties we can compare are magnetic field strength and morphology. Luckily, these two characteristics present enough puzzles to keep dynamo modelers busy. In Sect. 3 we review both non-magnetic and magnetic convection models for the giant planets. These planets provide us with additional model constraints in the form of observations of fluid flows in the outer layers of the planet. In Sect. 4 we discuss the known satellite dynamos and in Sect. 5 we conclude with a discussion of the current status and future of planetary dynamo modeling.

2 Terrestrial Planet Dynamos

The four terrestrial planets present a complete spectrum of dynamo states. Earth has a presently active dynamo generating an axial-dipole dominated field and paleomagnetic studies demonstrate that the dynamo has been around for at least the last three billion years. In contrast, Earth's sister planet Venus does not presently have an active dynamo, nor any evidence for remanent crustal fields implying dynamo action in its past, although better data will be required to completely rule out crustal magnetism on Venus. It is surprising that these two planets, so similar in internal structure and composition, present such different dynamo states. This difference is most likely due to the planets' abilities to cool their cores, clearly demonstrating the importance of the mantle in driving the dynamos.

The two smaller terrestrial planets, Mercury and Mars, have evidence for dynamo action sometime in their histories (Mercury currently and Mars in its early history). Both planets present magnetic mysteries which dynamo modelers must address and we discuss each planet individually below.

2.1 Mercury

Mercury's magnetic field was observed during the first and third flybys of the Mariner 10 mission in the mid-1970's (Ness et al. 1975, 1976). Recent flybys of Mercury by the MESSENGER spacecraft have confirmed these measurements and fit the observations with a dipole moment of $\sim 230\text{--}290 \text{ nT}\cdot R_M^3$, where R_M is Mercury's radius (Anderson et al. 2008). Little information on Mercury's magnetic field morphology is presently available aside from the dipole moment and possibly, the quadrupole moment, but more constraints are likely once MESSENGER begins taking measurements from orbit in 2011. Libration observations demonstrate that Mercury's core is at least partially liquid, suggesting that the magnetic field may be the result of an active dynamo (Margot et al. 2007). Another possibility, that the field is a remanent crustal field, requires lateral inhomogeneities in the crust (Stephenson 1975; Srnka 1976; Aharonson et al. 2004). Due to the purpose of this article, we will only consider the active dynamo possibility here.

If we assume Mercury's dynamo works much like Earth's dynamo, we can estimate the expected strength of the resulting magnetic field in the core. Independent scalings based on energetics and magnetostrophic balance suggest that Mercury's dynamo would produce a core magnetic field intensity of the order $10^5\text{--}10^7 \text{ nT}$ (Stevenson 1987; Schubert et al. 1988). Assuming an Earth-like field partitioning between toroidal and poloidal magnetic fields, this implies Mercury's surface field should be of order $4 \times 10^3\text{--}4 \times 10^6 \text{ nT}$, much stronger than the observed value of $\sim 260 \text{ nT}$.

Dynamo models for Mercury have focused on explaining the weakness of the observed field. Some reasoning or mechanism is proposed for why Mercury's dynamo should be non-Earth-like, and models are constructed to demonstrate that the proposed mechanism can produce a weaker Mercury-like surface field.

Several models evoke core geometry in their reasoning. Stanley et al. (2005) demonstrate that dynamos operating in thin shells with sufficiently low Rayleigh numbers such that convection only onsets outside the tangent cylinder can produce weak surface fields. In these models, toroidal fields are maintained strong throughout the core by differential rotation between the inner and outer cores, but poloidal fields are inefficiently regenerated by the weak convection in the limited area outside the tangent cylinder (Fig. 1(a)). This results in a weaker observed surface field. This model allows the generation of a strong field dynamo, but a non-Earth like field partitioning between poloidal and toroidal fields, thereby explaining why the observed (poloidal) fields are weaker than anticipated.

Takahashi and Matsushima (2006) have also published thin-shell dynamo models that produce weak dipole surface fields, but the reason for the weak fields is different. In their models, when a sufficiently large Rayleigh number is used such that convection is vigorous inside the tangent cylinder, smaller-scale non-dipolar fields dominate in the core. Because the power in smaller-scale modes decreases with distance faster than larger-scale modes, the small scale modes are much weaker at the surface and the observed surface field is dominated by its weak dipole component (Fig. 1(b)). Although this appears to be a promising mechanism, one issue with the models is that the inner core is made electrically insulating. The authors state that when they use conducting inner cores in their models, stronger dipolar fields result, suggesting that Mercury may not be explainable with this mechanism.

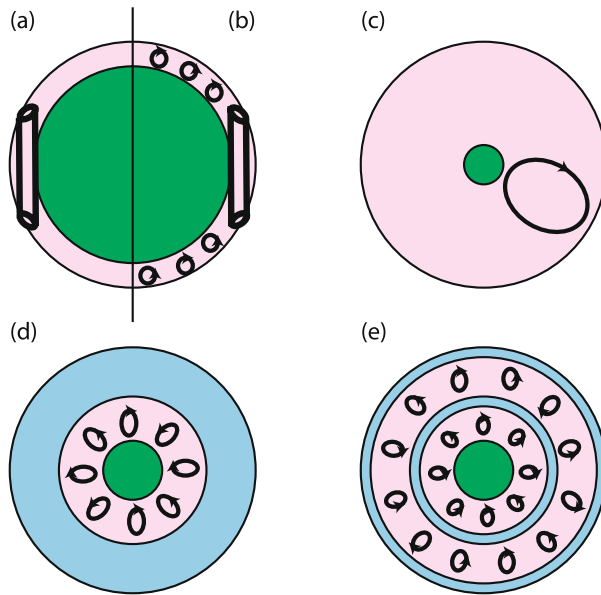


Fig. 1 Mercury dynamo model geometries. (a): Stanley et al. (2005) thin shell model with convection only outside the tangent cylinder, (b) Takahashi and Matsushima (2006) thin shell model with convection throughout the core, (c) Heimpel et al. (2005a) very thick shell model with isolated convection plume, (d) Christensen (2006) surrounding stable layer model, (e) Vilim et al. (2008) double dynamo model. A meridional slice is shown in (a) and (b) where the vertical line is the rotation axis, (c–e) are equatorial slices. The solid inner core is shown in green, stably-stratified layers are shown in blue and convectively unstable layers are shown in pink. In (a) and (b), long vertical cylinders represent the convection rolls outside the tangent cylinder whereas smaller circles represent the more 3-D convection pattern inside the tangent cylinder. In (c)–(e) slices of the convection rolls are represented as ellipses

At the other extreme in geometry, Heimpel et al. (2005a) rely on a very thick shell geometry to explain Mercury's weak observed field. Their numerical dynamo simulations which incorporate a very small solid inner core result in a single-plume mode of convection. This weaker convection generates weaker poloidal magnetic field explaining Mercury's weak observed surface field (Fig. 1(c)).

Other models for Mercury's weak surface field employ stable stratification (Christensen 2006; Christensen and Wicht 2008). Observations of Mercury's surface heat flow suggest it is possible that the outer portion of Mercury's core is thermally stratified and hence stable to convection. Numerical models which employ a thick outer stable layer in the core produce a weak surface field even though the field in the deep dynamo source region is strong (Fig. 1(d)). This is because the surrounding stable layer acts to attenuate the field through the skin effect, preferentially removing smaller-scale fields. Due to the slower rotation rate in Mercury, scaling laws suggest that Mercury's dynamo should be in the non-dipolar regime. Therefore, these models are affected both by the faster decay of the smaller scale features (since the dynamo operates deeper in the core) and the skin effect due to the stable layer.

Vilim et al. (2008) presents another Mercury model which relies on a non-Earth-like core stratification. Recent experiments have demonstrated that the Fe-S system produces non-ideal behaviour at Mercury-like pressures and temperatures for sulfur concentrations in the range 7–12 wt% (Chen et al. 2008). This non-ideal behaviour results in the dissolution of Fe from S at various locations in the core depending on the sulfur concentration. For

example, it is possible that Mercury's core is being driven by the freezing out of an Fe snow at either the outer boundary of the core or mid-way through the core, or both. If the layer is at mid-depth, then the freezing out of Fe also results in the release of a more buoyant S rich fluid above the layer which can also drive convection. Dynamo models operating in this geometry demonstrate that it is possible to reproduce Mercury's weak magnetic field through this mechanism (Fig. 1(e)). The two dynamo regions (one above and one below the mid-freezing layer) can drive dynamos that produce fields of opposite sign thereby diminishing the observed surface field strength.

Another model proposes a magnetospheric feedback mechanism to explain Mercury's weak surface field (Grosser et al. 2004; Glassmeier et al. 2007a, 2007b; Heyner et al. 2009). Because Mercury has a small magnetosphere (owing to its weak magnetic field) and is deeply embedded in the solar wind (owing to its proximity to the Sun), magnetospheric currents can generate significant magnetic fields affecting dynamo action in Mercury's core. Chapman-Ferraro currents, resulting from interactions between the internal dynamo and the solar wind, can generate an ambient field of order 50 nT at Mercury's surface. Kinematic dynamo models show that this ambient field is opposite in polarity to the field generated in the core, resulting in cancellation of field in the core. This mechanism is termed a "feedback" because the small magnetosphere results in these opposite polarity ambient fields which results in perpetuating the weak magnetosphere.

A thermoelectric dynamo was an early proposed alternative to the normal dynamo explanation for Mercury (Stevenson 1987; Giampieri and Balogh 2002). In this model, topography on the core-mantle boundary results in a poloidal thermoelectric current and associated toroidal field. Helical motions due to weak convection then act on the produced toroidal field to generate the weak observed poloidal field. Since this model does not rely on convection alone to drive the dynamo, it doesn't suffer from the same large scaling estimates for the intensity of the produced field. However, it does require good electrical conductivity of the lower mantle for the thermocurrents to close. It would be interesting to see numerical simulations of a thermoelectric dynamo to determine the feasibility of explaining Mercury's magnetic field.

When Mercury's magnetic field was first observed, it was difficult to explain the field through a dynamo mechanism. It now appears that several mechanisms are possible, so the current problem is distinguishing which mechanism is operating in Mercury. Determining Mercury's inner core size from upcoming observations will be challenging and so it will be difficult to eliminate potential dynamo mechanisms by gathering independent (not related to magnetic field) data on Mercury's core geometry. However, it may be possible to distinguish between the different mechanisms by examining characteristic features of the resulting magnetic field such as the observed surface magnetic power spectrum, locations of strong flux spots, and secular variation. Future data from the MESSENGER (Zuber et al. 2007) and Bepi-Colombo (Wicht et al. 2007) missions may therefore be able to distinguish between the models.

The dynamo models make various predictions for the surface magnetic power spectrum. The Stanley et al. (2005) thin shell model and Heimpel et al. (2005a) thick shell model produce significant power in the dipole and quadrupole components whereas the Vilim et al. (2008) double-dynamo model produces larger octupole power compared to the quadrupole mode. The Takahashi and Matsushima (2006) model produces strong power in several non-dipolar modes, whereas the Christensen (2006) model has little power in any mode but the dipole and quadrupole. The thermoelectric dynamo power spectrum depends on the scale of topography on the CMB.

Information may also be gathered by the location and secular variation of small-scale flux spots. Small scale intense flux spots are limited to equatorial regions in the Stanley et

al. (2005) and Vilim et al. (2008) models. In contrast, the Heimpel et al. (2005a) thick shell model produces strong normal flux spots at higher latitudes. These models also experience secular variation. The Christensen (2006) model suggests the fields should have little energy in higher harmonics and very slow secular variation due to the skin effect of the surrounding stable layer.

2.2 Mars

Mars' remanent crustal magnetic field, globally mapped by Mars Global Surveyor (Acuna et al. 1999), is most likely the result of an active dynamo in Mars' early history. Several mysteries surround the field including its hemispheric difference in field strengths, the magnetic carriers in the rocks and the driving force and timing of the dynamo. It is most likely that the dynamo was active sometime between 4.5–3.9 Ga since the large impact basins from the late-heavy bombardment (~ 3.9 Ga) are demagnetized, the majority of Tharsis (< 3.9 Ga) is demagnetized, and the ancient Martian meteorite ALH84001 has a magnetization age of 3.9–4.1 Ga (Weiss et al. 2002). Thermal evolution models have demonstrated that Mars could have maintained a super-adiabatic temperature gradient for millions to hundreds of millions of years sometime before 3.9 Ga if, for example, the core was initially superheated (Breuer and Spohn 2003; Williams and Nimmo 2004), magma ocean overturn resulted in the placement of cold cumulates at the core-mantle boundary (Elkins-Tanton et al. 2005), or plate tectonics was active in Mars' early history (Nimmo and Stevenson 2000).

If Mars possessed a super-adiabatic temperature gradient, then a past thermal dynamo is feasible. Other motions such as compositional convection as the inner core freezes and releases a light element (Stevenson 2001) or tidal motions due to interactions of Mars with an orbiting body (Arkani-Hamed et al. 2008) do not require a super-adiabatic core, further broadening the range of parameters for which an active dynamo could exist on early Mars. Martian interior models show that the core radius is approximately half the planetary radius, but aside from tidal Love numbers suggesting that some portion of the core is still liquid (Yoder et al. 2003), no information on the size of the solid inner core is available. Since Mars' dynamo has not been active since its early history, it is likely that it either has no inner core, or that the inner core is no longer growing.

Mars dynamo models are geared towards understanding the mysteries surrounding Mars' remanent magnetic field. A recent model addresses the difference in field intensity between the hemispheres (Stanley et al. 2008). Maps of the crustal magnetism demonstrate that the intensity of the fields correlate with the crustal hemispheric dichotomy. This suggests that whatever process produced the dichotomy in crustal thickness may be related to the dichotomy in magnetic fields. Both endogenic and exogenic formation scenarios for the crustal dichotomy have been presented in the literature. In the endogenic models, a degree-1 mantle circulation is responsible for the different hemispheric crustal thicknesses. This degree-1 pattern can result from a variety of scenarios such as mantle phase transitions (Weinstein 1995; Harder 1998; Breuer et al. 1998), radial viscosity variations in the mantle (Zhong and Zuber 2001; Roberts and Zhong 2006), magma ocean overturn (Elkins-Tanton et al. 2003, 2005) or boundary layer instabilities resulting from a superheated core (Ke and Solomatov 2006). In the exogenic models, a large glancing impact in the northern hemisphere is responsible for the excavation of northern hemisphere crust (Wilhelms and Squyres 1984; Frey and Shultz 1988; Andrews-Hanna et al. 2008; Marinova et al. 2008; Nimmo et al. 2008).

Both the endogenic and exogenic dichotomy formation scenarios have implications for the temperatures at Mars' core-mantle boundary (CMB). In the endogenic models, if the

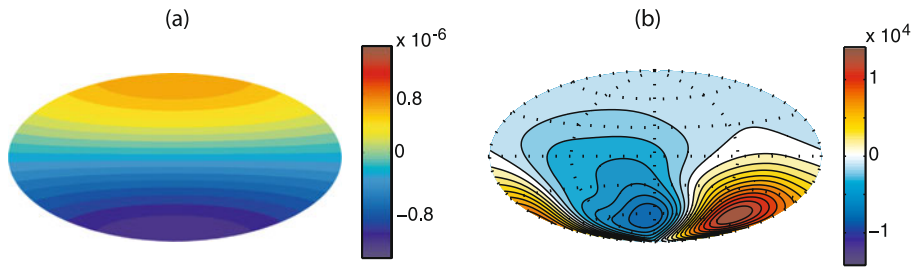


Fig. 2 (a): The degree-1 fixed heat flux boundary condition for the Stanley et al. (2008) Mars dynamo model. The superadiabatic heat flux is largest out of the southern hemisphere. Units are W/m^2 and a positive direction is into the core (hence outward heat flux at the CMB is negative). A thermal conductivity $k = 40 \text{ W}/\text{mK}$ was used to dimensionalize the superadiabatic heat flux in the models, however, dimensionalization is somewhat misleading due to the numerically unavoidable parameter regime used in the simulation. (b) The surface radial magnetic field for the Stanley et al. (2008) Mars dynamo model. Units are in nT

upwelling manifests in the northern hemisphere (resulting in basal crustal erosion and hence a thinner northern hemisphere crust) then the temperature on Mars' northern hemisphere CMB is hotter than in the southern hemisphere (where cold mantle material is falling onto the CMB). In the exogenic models, thermal perturbations due to the large impacts in the northern hemisphere can penetrate to the CMB under the impact (Watters et al. 2009). Both dichotomy formation scenarios can therefore result in a larger heat flux from the southern hemisphere CMB compared to the northern hemisphere CMB.

Stanley et al. (2008) implement the degree-1 CMB heat flux boundary variations implied by the dichotomy formation scenarios in a numerical dynamo model to determine the effects on the magnetic field (Fig. 2(a)). The result is a single-hemisphere dynamo where magnetic field generation is concentrated and strongest in the southern hemisphere. Due to the reduced heat flux from the northern CMB, the northern hemisphere of the core is sub-adiabatic and convection is most strongly driven in the southern hemisphere. The strong thermal winds in the model break the Proudman-Taylor constraint (Proudman 1916; Taylor 1917), although in the southern hemisphere, signs of rotational influences are still present. The resulting surface magnetic field is non-dipolar, non-axisymmetric and stronger in the southern hemisphere (Fig. 2(b)). This suggests that the reason Mars' crustal magnetic field is concentrated in the southern hemisphere may be because the dynamo produced strongest fields in the southern hemisphere.

The cessation of the Martian dynamo is another mystery that dynamo modelers have addressed. It is generally assumed that dynamo action ceased when the driving forces weakened enough such that the Rayleigh number became sub-critical. However, dynamo analytics (Childress and Soward 1972) show that a sub-critical dynamo is possible in the "strong field" regime where the Coriolis, Lorentz and buoyancy forces balance in the momentum equation. Essentially, the inhibiting effects of rotation and magnetic fields can offset each other resulting in convection at Rayleigh numbers below the critical value if only rotation were present. Recently, Kuang et al. (2008) produced sub-critical dynamo action in a spherical shell model suggesting that Mars' dynamo may have lasted longer than age estimates based on requiring a super-critical Rayleigh number. Their models also demonstrate that once the driving force decreases below the threshold for dynamo action in the sub-critical regime, it is unlikely to start up again unless the Rayleigh number increases by about 25 percent, suggesting it is hard to restart the dynamo. Their Mars dynamo, which maintains a relatively strong axial-dipolar dominated field in the super-critical regime, becomes more non-dipolar with frequent reversals in the sub-critical regime.

Another possibility for the termination of the Martian dynamo was suggested by Glatzmaier et al. (1999). The Mars dynamo may have ended by going through a series of dipole reversals and not completely recovering after each one. This occurs in one of their dynamo simulations that has a heat flux imposed at the CMB that is greatest at mid-latitude and least at the equator and poles (note that this is a different CMB heat flux variability than that of the Stanley et al. (2008) work discussed above). After several hundred thousand years with a strong magnetic field (starting with a homogeneous CMB heat flux condition) this case experiences a spontaneous dipole reversal with the usual drop in magnetic dipole intensity but fails to fully recover to the original field intensity after the reversal. Roughly a hundred thousand years later it reverses again and again recovers only to about 10% of its pre-reversal integrated magnetic energy. The unfavorable CMB heat flux condition, which forces more heat to be convected to mid-latitude instead of the preferred equatorial and polar regions, apparently destroys the more efficient fluid flow patterns for the dynamo mechanism.

3 Giant Planet Dynamos

All four of our solar system giant planets possess active dynamos, but the fields produced by the gas giants are markedly different from the ice giant fields. Whereas Jupiter and Saturn possess axial-dipole-dominated fields, Uranus' and Neptune's fields are dominated by multipolar components without a preference for axisymmetry (Connerney 1993). Aside from this difference in field morphologies, other mysteries surrounding the giant planet magnetic fields include:

- What mechanism is responsible for the zonal bands in the giant planet atmospheres, do they represent deeper zonal flows that play a role in dynamo generation, and why are they different for the different planets?
- Why is Saturn's dynamo producing such an axisymmetric field?
- How can Uranus and Neptune be generating magnetic fields with such low surface heat flows?

3.1 Overview of the Different Types of Models for Giant Planets

Most studies of the internal dynamics of giant planets have focused on explaining the maintenance of the observed surface flows and predicting the structure and extent of these flows below the surface. The flows in the deep interior, where the fluid is electrically conducting, maintain magnetic fields by shearing and twisting the existing field at a rate sufficient to offset magnetic diffusion. Since density increases with depth, convective velocity decreases with depth and electrical conductivity increases with depth (for our solar system giants). Therefore, magnetic induction by the flows and the resulting Lorentz forces on the fluid are mainly important within a range of depths in a giant planet where fluid velocity and electrical conductivity are both sufficiently large.

To be credible, a dynamo simulation of convection and magnetic field generation in the outer part of a giant planet should at least produce fluid flows near the non-conducting surface similar to those observed on the particular giant planet being simulated. This provides a valuable constraint that, for example, those who simulate convective dynamos in terrestrial planets do not have. To test how realistic are the flows and fields well *below* the surface in a dynamo simulation one can check if the total rate of entropy production by ohmic heating within the convection zone

$$\int (J^2/\sigma T)dV \quad (6)$$

is, on average, no larger than the rate entropy flows out at the top minus the rate it flows in at the bottom of the dynamo region, i.e., no larger than the *observed luminosity* times $(T_{top}^{-1} - T_{bot}^{-1})$ (Backus 1975; Hewitt et al. 1975). Here, J is the simulated electric current density and σ and T are the prescribed electrical conductivity and temperature, respectively.

We will therefore first review some non-magnetic modeling studies of fluid flows in giant planets before discussing simulations of dynamically-consistent convective dynamos. There have been several two dimensional (2D) modeling studies of vortices in the shallow atmosphere of giant planets. However, since we are interested in planetary dynamos, here we consider only three-dimensional (3D) global simulations. We will also focus on zonal winds (i.e., the axisymmetric part of the longitudinal velocity) because they dominate the flow at the surface and because their extension into the semi-conducting region below the surface plays a critical role in maintaining the toroidal magnetic field.

The surface zonal winds on our giant *gas* planets, Jupiter and Saturn, advect the latitudinally-banded clouds observed on the surfaces of these planets (Sanchez-Lavega et al. 2002; Porco et al. 2003). These longitudinally-averaged winds alternate in latitude between eastward directed (i.e., prograde) and westward directed (i.e., retrograde) relative to a rotating frame of reference (Fig. 3), which is chosen to be that of the global magnetic field based on observed radio emissions. Note, that this reference frame does not represent the mean angular velocity at the cloud tops nor the rotating frame in which the total angular momentum of the planet vanishes. It also does not necessarily represent the average angular velocity of the deep interior. It approximates the mean angular velocity of the region in which the dynamo operates and could have a phase velocity relative to this region. In addi-

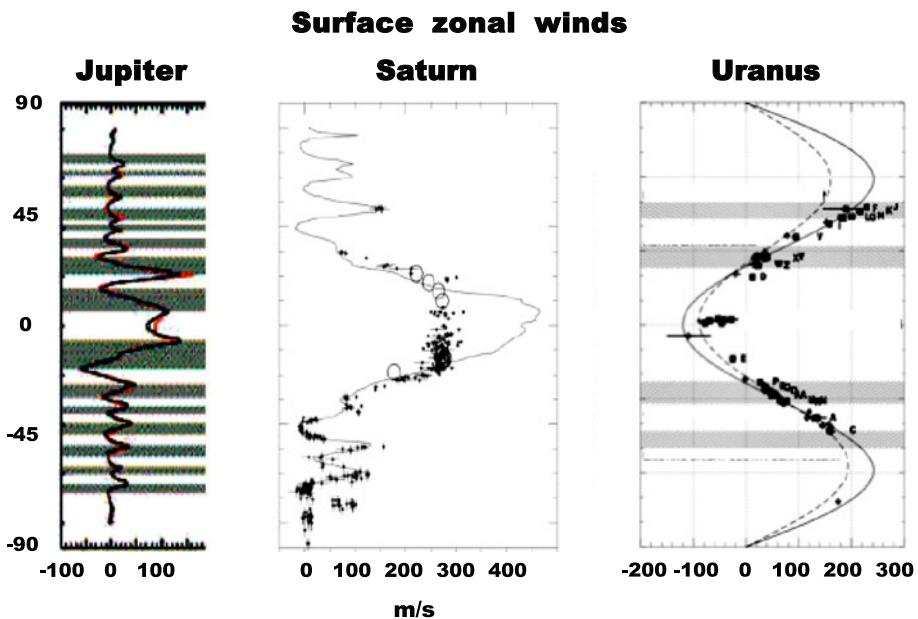


Fig. 3 Plots of the observed zonal winds vs. latitude on Jupiter, Saturn and Uranus. Positive velocities are prograde; negative are retrograde. *Hubble Space Telescope* measurements (*dots*) of Saturn's zonal winds from 1996–2002 show that the peak equatorial jet has decreased by roughly a factor of two since the measurements by the *Voyager Mission* (*solid line*) from 1980–1981. (Sanchez-Lavega et al. 2002; Porco et al. 2003; Hammel et al. 2005)

tion, like the magnetic fields in the sun and the Earth, it is not necessarily constant in time (Giampieri et al. 2006) because the field is maintained by time dependent magnetohydrodynamics. The equatorial jets on Jupiter and Saturn are prograde relative to this chosen frame of reference. Although the zonal wind pattern on Jupiter has been fairly constant for the past three decades, the intensity of the equatorial jet on Saturn has decreased by roughly a factor of two since the time of the *Voyager Mission* (Fig. 3). This may have been an actual change in wind speed or a change in the level of the clouds, which are measured to calculate the speed.

The *ice* giants, Uranus and Neptune, also display a surface differential rotation rate in latitude. However, unlike the gas giants and more like the zonal winds in the Earth's atmosphere, they have a broad retrograde equatorial jet and only one prograde zonal flow at high latitude in each hemisphere (e.g., Hammel et al. 2005).

Many attempts have been made to explain the maintenance of these surface zonal wind patterns and predict their amplitudes and patterns below the surface, i.e., the differential rotation. They can be maintained by Coriolis forces resulting from a thermally-driven meridional circulation (i.e., a "thermal wind") or by the transport of longitudinal momentum by radial and latitudinal flows (i.e., the convergence of Reynolds stress). The axisymmetric parts of viscous and magnetic forces also play a role; however, these forces usually inhibit differential rotation in planets.

Most studies of zonal winds in giant planets have come from two scientific modeling groups: the atmospheric climate modeling community and the geodynamo and solar dynamo modeling communities. Both groups have attempted to use modified versions of their traditional computer models. Modelers from the atmospheric community usually prescribe an atmosphere stratified in density and temperature based on estimates of what these are for the relevant planet. However, their global models are based on the assumption that the observed surface winds are maintained exclusively by the dynamics within the very shallow weather layer. The "shallow-water" model simplifications are based on large-scale horizontal flows and ignore the small-scale buoyantly-driven flows in radius. For reviews of (non-magnetic) climate models see, for example, Dowling (1995) and Showman et al. (2007).

By placing an impermeable lower surface just below the clouds, as is the case for the Earth, these atmospheric models completely ignore the convection in the deep interiors of these fluid bodies. The *Galileo* probe, however, measured strong zonal wind down to a pressure of 20 bars, well below the weather layer driven by solar insolation, with no indication of the wind becoming weaker with depth (Atkinson et al. 1998). The existence of a global magnetic field provides indirect evidence of significant flows at much greater depths. That is, since the magnetic dipole decay time for a body with the size, electrical conductivity and temperature of Jupiter's deep interior is roughly only a million years, a dynamo likely exists in its electrically-conducting interior, driven by deep convection and zonal winds.

Modelers from the geodynamo community use 3D deep convection models to investigate the structure and maintenance of zonal winds (i.e., differential rotation) without making shallow-water type approximations. However, most have assumed no stratification of density, a fairly good approximation for the Earth's fluid core but not for the outer regions of giant planets. A few studies, however, do account for both deep convection zone and large density stratification, similar to modeling studies that have been conducted in the solar dynamo community for the past quarter century. Although these models capture more of the correct physics of the problem, they too need improvements. See, for example, Dormy et al. (2000), Kono and Roberts (2002) and Glatzmaier (2002) for reviews of the geodynamo models.

The shallow-atmosphere community and the deep-convection community have mostly ignored each other and have seldom referenced each others papers. However, since deep-convection *dynamo* models are being judged on their ability to maintain banded zonal winds at their outer boundaries like those observed in the shallow cloud layers of our gas giants, it is important to discover and understand the mechanism that maintains these winds. In particular, it is important to know if this mechanism is seated mainly within the shallow atmosphere, as the atmospheric community claims, or mainly within the deep convection zone as claimed by that community. A critical issue for studies of our solar system giant planet dynamos is to know the depth to which the strong winds penetrate. Also, although the outer atmospheres of our gas giants are relatively cold and have very low electrical conductivity, the outer atmospheres of the extrasolar gas giants in close orbit around their parent stars are probably partially ionized by the stellar radiation. Therefore, the structures of the flows in these electrically conducting atmospheres is very important for studies of the surface dynamos of these planets.

The very different approaches and approximations to modeling the internal dynamics of giant planets have several subtle, but seldom discussed, effects on the respective results. We discuss the resulting deficiencies below as we describe some of the non-magnetic modeling results. Then we discuss some simulations of convective magnetohydrodynamic (MHD) dynamos for gas giants and ice giants. These dynamically self-consistent solutions of thermal convection and magnetic field generation have only been produced using deep convection models.

3.2 Atmospheric Models

Some atmospheric models of giant planets rely on a thermal wind scenario (e.g., Allison 2000) for which a meridional circulation (the axisymmetric north-south flow) drives the zonal winds (the axisymmetric east-west flow) via Coriolis forces. That is, axisymmetric flow toward the equator moves fluid further away from the planet's rotation axis, increasing its moment of inertia, and, to the extent that angular momentum is conserved, causes its angular velocity to decrease. Likewise, flow toward a pole increases the fluid's angular velocity. This naturally results in a retrograde zonal wind in the equatorial region relative to the global mean angular velocity (e.g., Williams 1978; Cho and Polvani 1996), as is the case for the Earth's lower atmosphere and for our ice giants. Note, that a latitudinally-banded pattern of zonal winds with a prograde equatorial jet can be obtained by tuning a prescribed heating function distributed in latitude and radius that continually nudges the temperature toward a profile that drives the desired zonal wind pattern (e.g., Williams 2003). However, such mathematical fits to surface observations do not provide a dynamically-consistent prediction or explanation for the maintenance of an observed zonal wind structure.

Some of the most sophisticated gas giant modeling attempts within the atmospheric community have been made using general circulation models (GCMs). These 3D global models, which were originally designed and used for studies of the Earth's climate and weather, represent a shallow spherical shell of density-stratified gas with a depth less than a percent of the planetary radius. They typically parameterize the radiation transfer using a Newtonian heating/cooling method, which simply nudges the local temperature toward a prescribed temperature profile based on an assumed timescale. GCMs also have "shallow-water" simplifications based on the assumption that the length and velocity scales in radius are small compared to those in the horizontal direction. For example, they assume local hydrostatic equilibrium instead of solving the radial component of the full momentum equation. That is, the radial pressure gradient is forced to always exactly balance the weight of the

fluid above. Consequently, the Coriolis, buoyancy and viscous forces and the divergence of Reynolds stress are all neglected in the radial direction. Therefore, instead of evolving the radial component of the fluid velocity via the momentum equation, as is done for the horizontal components, it is calculated by determining what it needs to be to satisfy mass conservation, hydrostatic balance and the equation of state once the horizontal divergence of the horizontal flows is updated (at each grid point and time step).

This has worked sufficiently well for GCMs used to study the large scale flows in the Earth's atmosphere. However, the Earth's atmosphere *does* have an impermeable lower boundary; the atmosphere of a giant planet, on the other hand, extends smoothly into a dense, convecting interior (e.g., Bodenheimer et al. 2003; Guillot 1999). The radial velocity associated with such a grid cell in a GCM represents the spatial average of many, much stronger, small-scale up and down drafts within the entire cell; it is not meant to be a representative value of the actual dynamical velocity in the Earth's atmosphere. When averaged this way, these radial velocities are small relative to the horizontal winds. Therefore, most GCMs also neglect the contribution to the Coriolis and Reynolds stress terms in the *longitudinal* component of the momentum equation that are due to radial velocity.

Solving for the radial flow via the divergence/convergence of horizontal flows, instead of driving it with buoyancy and Coriolis forces, misses critical aspects of the dynamics of deep rotating convection. This is apparent in profiles of the flow and temperature produced by giant planet GCMs for which vortices parallel to the planetary rotation axis are not prominent; such vortices are a dominant feature of flows seen in laboratory experiments and 3D simulations of deep rotating convection. In addition, inertial oscillations, which are driven by Coriolis restoring forces, are also poorly represented in GCMs because of the neglect of Coriolis forces in radius due to longitudinal flows and in longitude due to radial flows. The neglect of buoyancy to drive radial velocity and the neglect of Coriolis and Reynolds stress terms involving the radial velocity have prevented GCM studies from self-consistently producing prograde equatorial zonal winds.

Lian and Showman (2009) have recently produced much more promising GCM simulations that model the effects of moist convection. Although moist convection is highly parameterized in their model, it increases the vigor of the radial flows by releasing latent heat where water vapor condenses. That is, when fluid containing water vapor is advected upward it condenses at some lower-temperature level and releases latent heat. This causes thermal expansion and horizontal divergence, which pulls up more fluid. Unlike previous GCM simulations, their model can produce, without prescribing ad hoc heating patterns, banded zonal surface flows with a prograde equatorial jet (Fig. 4) qualitatively similar to those of our gas giants. These profiles are maintained due to the convergence of Reynolds stress, including that due to the product of radial and longitudinal velocities, which previous GCM studies have neglected. They argue that the latitudinal widths of the zonal wind bands are determined by a "Rhines effect" (Rhines 1975), which predicts a local length scale proportional to the square root of the zonal wind speed. This arises when the advection in latitude of radial vorticity is balanced by the generation of radial vorticity due to the latitudinal gradient of the radial component of the planetary rotation rate.

Lian and Showman (2009) can also produce a retrograde equatorial jet (Fig. 4), like those of our ice giants, when they prescribe a larger source of water vapor, which effectively increases the vigor of the convective flows. The change from prograde to retrograde zonal flow in the equatorial region when convective driving increases relative to Coriolis effects has been demonstrated in deep convection models and shown to also depend on the ratio of viscous to thermal diffusion and on the degree of density stratification (Glatzmaier and Gilman 1982). Although the Lian-Showman model still suffers from the hydrostatic shallow-water

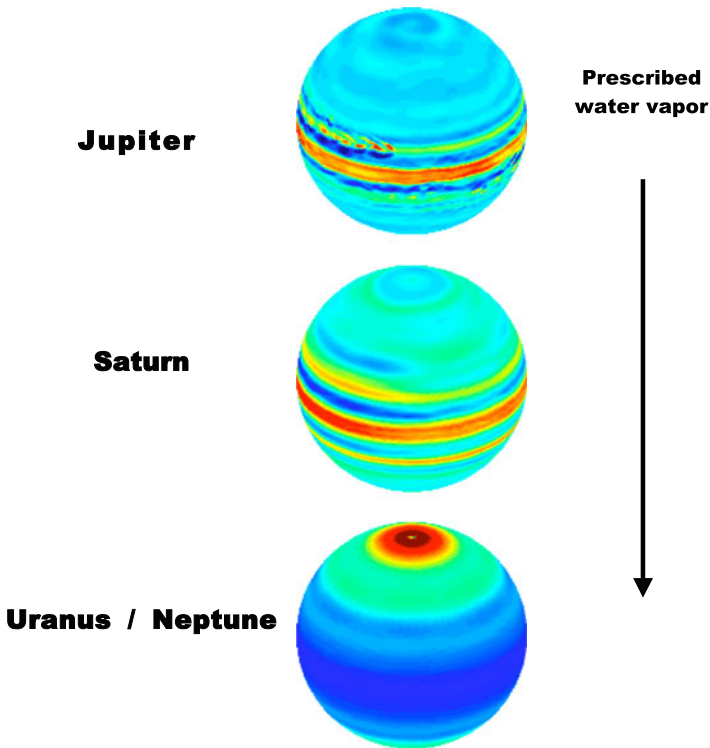


Fig. 4 Snapshots of the longitudinal velocity in GCM simulations with moist convection. *Reds* represent prograde winds; *blues* retrograde. These simulations vary, from “Jupiter” to “Uranus/Neptune” by increasing the amount of prescribed water vapor in the model. (Lian and Showman 2009)

simplifications mentioned above, it is beginning to capture some of the important dynamics seen in 3D deep convection models.

3.3 Non-magnetic Deep Convection Models

It may be the case that the zonal winds on giant planets are confined to the shallow surface layers and driven by heat sources and moist convection there without significant influence from the deep convection below. However, hydrostatic shallow-water type models, including GCMs, assume this from the start instead of allowing the full dynamics to demonstrate it. Deep convection models can also produce banded zonal winds with either prograde or retrograde equatorial jets, without neglecting the dynamics of the deep interior. They are designed to capture the 3D dynamics within a deep rotating fluid shell but not necessarily the 2D dynamics in a shallow atmosphere. Therefore, they neglect moist convection and approximate radiative transfer as a thermal diffusive process.

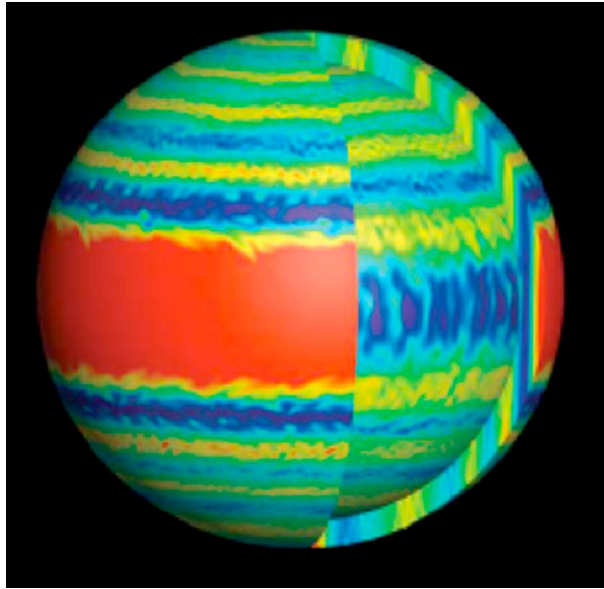
The deep convection models of the geodynamo and solar dynamo communities are what the atmospheric community would call “non-hydrostatic” models. That distinction is not made in the dynamo communities because all 3D convection and dynamo models are non-hydrostatic. There was never a reason to make shallow-water type approximations for these models because the convection zone depths for the geodynamo and solar dynamo are comparable to the radii of the respective bodies, as they are for giant planets. Therefore, all three

components of the momentum equation are solved, putting the radial component of velocity on the same footing as the horizontal components. This is really needed to capture the full dynamics of deep rotating convection; i.e., the entire Coriolis force and Reynolds stress are used and the buoyancy force drives convection.

The full representation of these forces in deep convection models captures the generation of vorticity parallel to the planetary rotation axis as fluid moves relative to this axis. When Coriolis and pressure gradient forces nearly balance everywhere and all other forces are relatively small, the classic Proudman-Taylor theorem (Proudman 1916; Taylor 1917) predicts that rotating, incompressible, laminar fluid tends to flow within planes parallel to the equatorial plane. Within such a convective column or vortex, rising fluid generates negative vorticity relative to the rotating frame of reference and sinking fluid generates positive vorticity. This results in a prograde-propagating Rossby-like wave because positive vorticity is generated on the prograde sides of positive vortices and likewise negative vorticity is generated on the prograde sides of negative vortices. Since the effect is greatest near the surface, rising fluid parcels within the vortices curve to the east and sinking curve to the west. This causes rising fluid to be correlated with eastward flow and sinking fluid to be correlated with westward flow. The resulting convergence of this nonlinear Reynolds stress maintains a zonal wind (i.e., differential rotation) with a prograde equatorial jet near the surface. In such a case, a meridional circulation, much weaker than the zonal wind, is maintained by the Coriolis forces resulting from the zonal wind. If, on the other hand, buoyancy forces dominate over Coriolis forces, the curving of rising and sinking fluid is much less correlated and the thermal wind, with a retrograde equatorial jet, is maintained by Coriolis forces resulting from the meridional circulation (e.g., Glatzmaier and Gilman 1982; Aurnou et al. 2007). Of course this assumes convective velocities are large enough to make a relatively significant Reynolds stress. If they are not, as is the case for the geodynamo, the zonal flow in the equatorial region tends to be retrograde even if Coriolis forces dominate over buoyancy forces (e.g., Kono and Roberts 2002).

Two basic types of deep convection models have been used to study giant planets: those that ignore the background density stratification and assume a liquid equation of state (Boussinesq models) and those that account for density stratification and use a gas equation of state (anelastic models). There is a fundamental difference between the way these two types of models maintain differential rotation. Models that assume a constant background density rely on the classic vortex-stretching mechanism (Busse 1983, 2002) to generate vorticity and maintain differential rotation. This relies on the existence of convective columns aligned parallel to the planetary rotation axis and spanning from the outer (impermeable) surface in the northern hemisphere to that in the southern hemisphere. Negative vorticity (i.e., an anti-cyclone) is generated in rising fluid (within such a column when outside the tangent cylinder to the inner boundary) because conservation of mass and incompressibility require rising fluid to spread out normal to the axis as it approaches the sloping impermeable outer boundary. The resulting Coriolis torque generates the vorticity, which drives a prograde propagating Rossby-like wave (as described above) because of the spherical shape of the outer boundary. Likewise, sinking fluid is stretched parallel to the axis because of the sloping boundaries, generating positive vorticity (i.e., a cyclone). Under the special geostrophic conditions mentioned above, with enough viscosity to maintain relatively laminar flow and large diameter columns, this mechanism is able to maintain differential rotation via the convergence of Reynolds stress as explained above (e.g. in simulations: Gilman and Miller 1981; Christensen 2002; Heimpel et al. 2005b; and in laboratory experiments: Busse and Carrigan 1976; Hart et al. 1986; Manneville and Olson 1996; Aubert et al. 2001; Aurnou 2007).

Fig. 5 A snapshot of the longitudinal winds maintained on the outer and inner boundaries in a simulation of Jupiter using a Boussinesq, deep rotating convection model. *Reds* represent prograde winds; *blues* retrograde. (Heimpel et al. 2005b)



Most published studies of convection in giant planets have been based on the Boussinesq approximation and most have simulated only the outer 10 to 20% in radius of the planet (see papers by Wicht and Tilgner and by Christensen in this issue). The resulting differential rotation manifests itself on the surface as a zonal wind, beautifully-banded in latitude, with a strong prograde equatorial jet qualitatively similar to those of Jupiter and Saturn. An example by Heimpel et al. (2005b) is shown in Fig. 5.

Heimpel et al. (2005b) argue that the widths of the bands in latitude are determined by a modified “Rhines effect” due to the approximate balance of the advection of vorticity by zonal wind and the stretching of fluid along the axes of convective columns due to the spherical geometry of the outer impermeable boundary. This Coriolis stretching effect decreases with latitude, unlike the Coriolis effect of shallow-water GCMs. Therefore, this mechanism maintains a *prograde* equatorial jet. According to the authors, the location of the inner impermeable boundary in their model determines the width and amplitude of the equatorial jet.

In addition to the prograde equatorial jets of Jupiter and Saturn, the retrograde equatorial jets of Uranus and Neptune have been investigated using Boussinesq deep convection models. Aurnou et al. (2007) show that the direction of the equatorial jet in their models depends on the relative importance of Coriolis and buoyancy forces as Glatzmaier and Gilman (1982) demonstrated with anelastic models. As discussed above, when Coriolis forces dominate over buoyancy forces a prograde equatorial jet, similar to those seen on the gas giants, is maintained. If instead buoyancy forces become comparable to or exceed Coriolis forces, a retrograde equatorial jet is maintained.

Although beautiful results have been obtained by these deep-convection constant-density simulations, an obvious question is how realistic is the simulated structure of the convection and the maintenance of differential rotation when density stratification is ignored. The density in giant planets varies in radius by many orders of magnitude, especially in the outer part of the planet (e.g., Bodenheimer et al. 2003; Guillot 2005). For the Boussinesq approximation to be valid, the depth of the convection zone needs to be small relative to the

local density scale height. However, since the top of the convection zone is at a pressure of roughly 1 bar, Jupiter's outer 10% in radius, for example, spans about eight density scale heights. That is, the expansion of rising fluid and contraction of sinking fluid have first-order effects on the fluid flows in the outer regions of giant planets. In addition, because the interiors of giant planets have very small viscosity, convective columns (vortices) in these planets likely have extremely small diameters and the flows are probably strongly turbulent, not laminar. Under these conditions, it is unlikely that such long thin convective columns would develop and stretch uniformly while spanning many density scale heights from the northern to southern boundaries (Glatzmaier et al. 2009). Instead, many short, disconnected vortices or vortex sheets would likely exist, on which the sloping outer boundary would have little effect.

To capture the effects of a significant density stratification and a gas equation of state, for which density perturbations depend on both temperature and pressure perturbations, some deep convection models employ the anelastic approximation. As for GCMs and Boussinesq models, sound waves are naturally filtered out in anelastic models in order to use much larger numerical time steps. This approximation to the fully compressible system of equations is valid when the fluid velocity is small compared to the local sound speed and thermodynamic perturbations are small relative to the mean (spherically symmetric) profiles, as is likely the case within giant planets. Background (reference state) profiles in radius of density, temperature and pressure are prescribed that are hydrostatic and usually adiabatic; this reference state may also evolve in time. The 3D time-dependent thermodynamic perturbations, which are neither hydrostatic nor adiabatic, are solved relative to this state. Various initial reference states have been employed: for example, polytropic solutions to the Lane-Emden equation (e.g., Hansen and Kawaler 1994) and polynomial fits to one-dimensional evolutionary models of giant planets (e.g., Guillot 2005). The equation of state for the outer part of a gas giant can be approximated as a perfect gas, i.e., reference state pressure is proportional to density times temperature. However, the deep interior is a non-relativistic degenerate electron gas (e.g., Guillot et al. 2004), with reference state pressure proportional to density to the 5/3 power (e.g., Hansen and Kawaler 1994).

Recently Jones and Kuzanyan (2009) produced anelastic simulations to study the internal convection and differential rotation of density-stratified gas giants. In one of their studies they compare solutions in the outer 30% in radius; one case spans five density scale heights (i.e., a factor of 148 in density) and another spans only a tenth of a scale height (essentially Boussinesq). Both of these cases have a broad equatorial prograde jet, with relatively little zonal wind at higher latitudes (Fig. 6). They clearly demonstrate the effects of density stratification. In the strongly stratified case the amplitude of the convection and differential rotation decrease significantly with depth; whereas the amplitudes are much more uniform in depth for the nearly constant density case.

One of us (Glatzmaier) has simulated the internal dynamics of giant planets using a modified version of an anelastic solar dynamo model (Glatzmaier 1984). Figure 7 shows snapshots of two recent anelastic simulations that use the same density background profile, which spans five density scale heights. These two cases also have the same thermal diffusivities and the same velocity and thermal boundary conditions. However, viscous diffusivity for case 2 is ten times smaller than that for case 1. This decrease in viscosity increases both buoyancy and Coriolis forces by roughly the same factor. The more viscous case (1) maintains a shallow prograde jet in the equatorial region with a peak velocity of 140 m/s (relative to the rotating frame) and essentially solid-body rotation inside a cylinder tangent to this jet (i.e., not tangent to the inner impermeable boundary); the amplitude of the convection drops two orders of magnitude from the outer to the inner regions. The more turbulent case (2) has

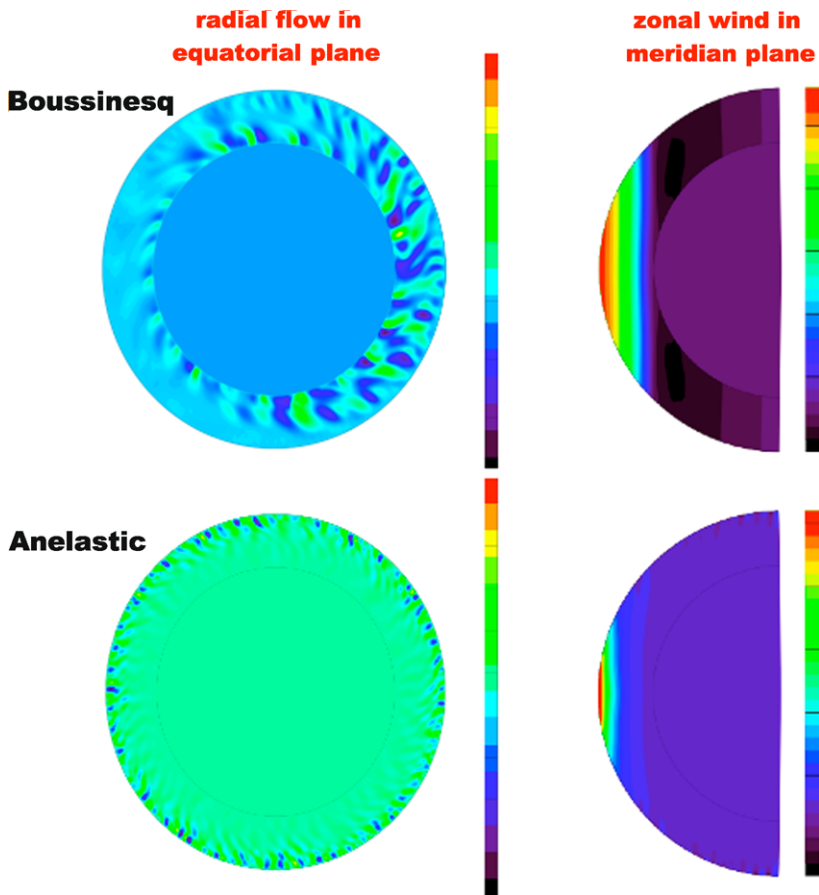


Fig. 6 Snapshots of the radial component of the convective velocity in the equatorial plane (*left*) and the zonal winds in the meridian plane (*right*) for two anelastic simulations. The *top row* is for a case that is nearly Boussinesq (spanning 0.1 density scale heights). The *bottom row* is a case with a significant density stratification (spanning 5 density scale heights). On the *right*, *green* is upflow and *blue* is downflow. On the *left*, *red* is prograde and *blue* is retrograde. (Jones and Kuzanyan 2009)

a deeper equatorial jet, which peaks at 470 m/s at the surface, and several weaker alternating zonal wind bands that penetrate the deep interior and extend to the poles; the convective amplitude drops only about one order of magnitude with depth. Jones and Kuzanyan (2009) see qualitatively similar results. Starchenko and Jones (2002) argue that the amplitude of the convective flows deep within gas giants should be about a cm/s or less in order to maintain roughly the same total convective heat flow as observed at the surface. One of their assumptions is that rising fluid is always hot and sinking is cold, which is reasonable for laminar convection. However, for strongly turbulent convection, especially when dominated by vortices, this need not be the case. Therefore, one could expect the average amplitude of the flows to increase, without increasing the net heat flow, when viscosity is decreased. This effect, however, may be greater near the surface where the flow is more turbulent.

Although long, thin and straight convective columns spanning the entire interior are not precluded in these anelastic simulations, they seldom develop when the flow is even weakly turbulent. Unlike the Boussinesq models, however, such structures are not needed

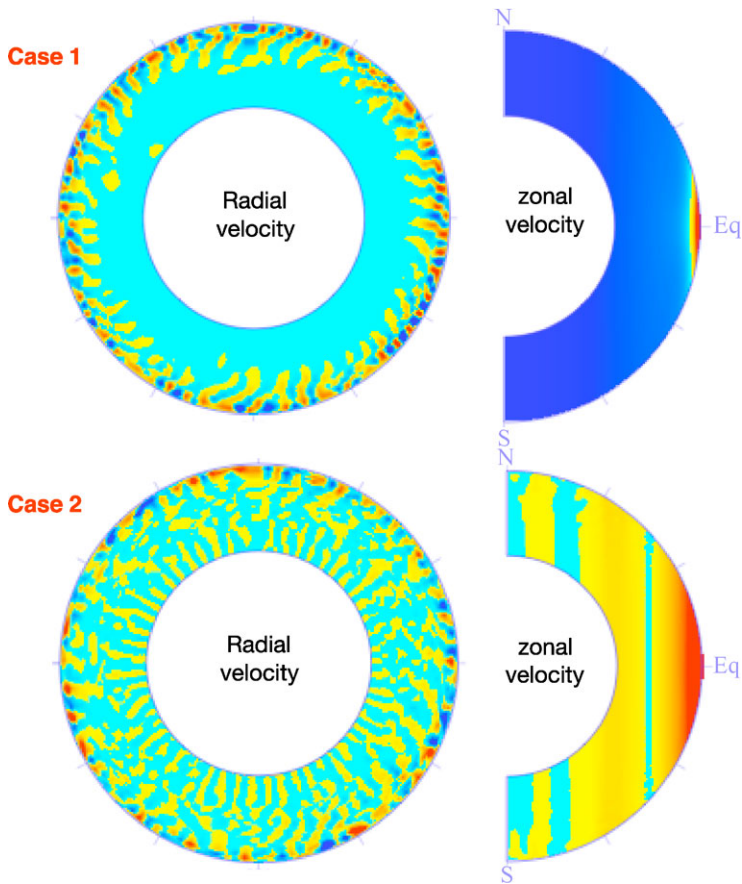


Fig. 7 Snapshots of the radial component of the convective velocity in the equatorial plane (*left*) and the zonal winds in the meridian plane (*right*) for two anelastic simulations, both spanning five density scale heights. Case 2 has viscosity ten times smaller than that of Case 1. *Reds* and *yellows* are upflow (*left*) and prograde (*right*); *blues* are downflows (*left*) and retrograde (*right*). (Simulations by G.A. Glatzmaier)

to maintain a differential rotation pattern with a prograde equatorial jet at the surface. That is, instead of being generated by a stretching torque, local vorticity (parallel to the planetary rotation axis) is generated mainly by compressional torque due to the expansion of rising fluid and contraction of sinking fluid (Glatzmaier and Gilman 1981; Glatzmaier et al. 2009). A prograde propagating Rossby-like wave is now driven because density decreases outward, not because the boundaries are spherical; and the persistent tilt in longitude of rising and sinking fluid, required for the convergence of prograde angular momentum in the surface equatorial region occurs because the density scale height decreases with increasing radius (at least in the gas giants). This mechanism for maintaining differential rotation exists even for short isolated vortices rising and sinking within strongly turbulent environments. The resulting pattern of differential rotation, in radius and latitude, depends on the details of the thermal, compositional and density stratifications in radius.

One important distinction to recognize is the difference between these *non-axisymmetric* convective vortices and the *axisymmetric* zonal flows centered on the planetary rotation axis (i.e., the “constant-on-cylinders” differential rotation). The former tend to be relatively small

scale; whereas the latter are broad and, at least in the equatorial region, do extend through the interior from the northern surface to the southern surface. This difference exists because the zonal flow has no component in radius and therefore does not experience the density stratification.

3.4 Magnetic Deep Convection Models

3.4.1 Gas Giants

Having discussed the various 3D simulations of convective structures and zonal flows that may occur in giant planets, we now consider the types of magnetic fields these flows of electrically-conducting fluid could maintain by shearing and twisting existing fields. Models of the geodynamo and solar dynamo typically prescribe a constant electrical conductivity. Several computational studies of dynamos in gas giants have also assumed a constant background density and electrical conductivity (see papers by Wicht and Tilgner and by Christensen in this issue). However, more realistic models of gas giants need to account for the large stratifications in density and electrical conductivity in the outer semi-conducting region, which have first order effects on the structure of the generated magnetic field. The electrical conductivity, for example, likely increases exponentially with depth before becoming constant below the molecular-metallic hydrogen phase transition (e.g., Guillot et al. 2004). That is, in the outer semi-conducting region magnetic diffusivity is not constant, but increases rapidly with radius (Liu et al. 2008).

The effects of significant stratifications in electric conductivity and density have been demonstrated in an anelastic dynamo simulation of a Jupiter-like planet (Glatzmaier 2005). This deep convection zone model spans the outer 80% in radius; the inner 20% is assumed to be a solid core. Constant viscous and thermal diffusivities are prescribed, with the ratio of viscous to thermal being 0.01. The prescribed electrical conductivity increases exponentially with depth by three orders of magnitude in the outer semi-conducting region, up to a constant value in the lower “metallic hydrogen” region. However, the amplitude of convection decreases with depth because of the density stratification. Therefore, magnetic energy is very small in the deep interior and instead peaks in the lower semi-conducting region, where electrical conductivity and convective velocity are both high enough to efficiently generate magnetic field. The results are sensitive to the number of density scale heights represented, the radial profile of electrical conductivity, the vigor of the turbulent convection and the relative effects of Coriolis forces.

Guided by this deep-shell anelastic simulation, Glatzmaier (2005) also simulated a shallower convective dynamo to study the dynamics of the semi-conducting region. Only the outer 20% of the planetary radius is simulated. This generic gas-giant model has a radius, a rotation rate and radial profiles of density, temperature and pressure that are roughly averages of what are obtained in one-dimensional models of Jupiter and Saturn (Guillot 2005). In terms of traditional non-dimensional parameters, the (classic) Rayleigh number is 10^9 , Ekman number is 5×10^{-7} and Prandtl number is 3×10^{-2} . The simulation spans about 6 years, more than 3,000,000 numerical time steps, the last half of these at a spatial resolution of 768 grid points in latitude, 768 in longitude and 241 in radius.

Due to the density stratification, the convective velocity near the transition depth is typically an order of magnitude smaller than it is near the surface and two orders of magnitude smaller than the surface zonal winds. Small-scale isolated vortex structures exist in the convection zone. Differential rotation persists throughout the convection zone as latitudinally-alternating angular velocity constant on cylinders coaxial with the rotation axis (Fig. 8).

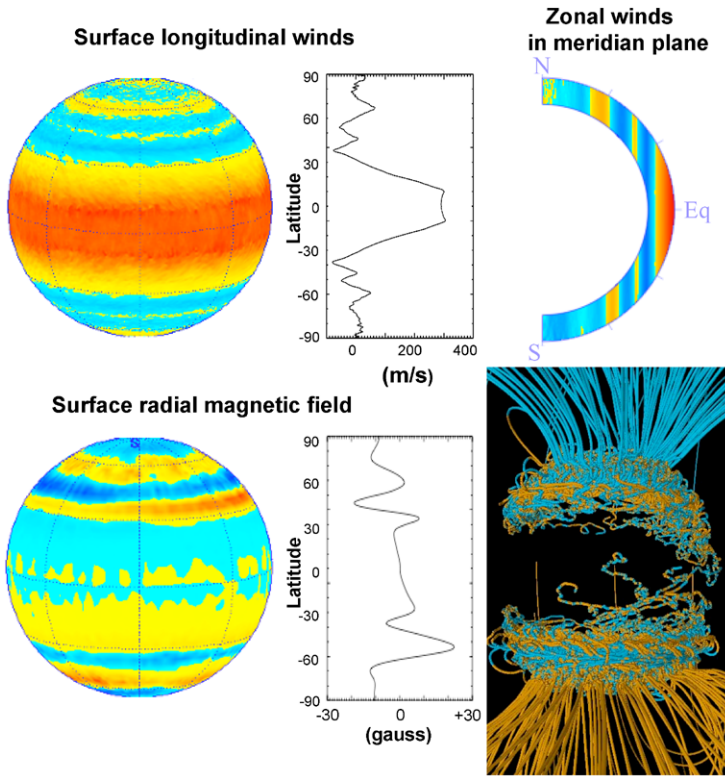


Fig. 8 Snapshots of an anelastic simulation of a gas giant dynamo. *Top row:* The longitudinal component of velocity at the surface, its zonal average vs. latitude and the zonal velocity displayed in the meridian plane. *Reds and yellows* are eastward up to 300 m/s; *blues* are westward relative to the rotating frame up to 100 m/s. *Bottom row:* The radial component of the magnetic field at the surface, its zonal average vs. latitude and the 3D field illustrated with lines of force. *Reds and yellows* are outward directed; *blues* are inward. *Orange lines* of force are directed outward; *blue* are directed inward. Typical intensity within the convection zone is a few hundred gauss. (Glatzmaier 2005)

This appears on the surface as a banded axisymmetric zonal wind profile. The differential rotation in radius is maintained by the density-stratification mechanism (Glatzmaier et al. 2009) because the density scale height decreases with radius, as discussed above. The peak zonal wind velocities at the surface decrease with latitude because the density scale height, measured normal to the rotation axis, naturally decreases with latitude. The strength and latitudinal extent of the equatorial jet at the surface (Fig. 8), which here is more like Saturn’s than Jupiter’s (Fig. 3), is sensitive to the prescribed density stratification, viscosity and the ratio of buoyancy to Coriolis forces. Maintaining a differential rotation profile more like Jupiter’s will likely require a more turbulent simulation, which would be achieved by decreasing viscosity while increasing spatial and temporal resolution.

Although convection kinetic energy peaks near the surface in this simulation, magnetic induction is most efficient in the lower quarter of the simulated convection zone where the electrical conductivity is greatest. There the differential rotation shears the poloidal field into toroidal (east-west) fields. To limit this shear (and the resulting ohmic dissipation), poloidal field tends to align parallel to surfaces of constant angular velocity, as suggested by Ferraro’s iso-rotation law (Ferraro 1937). This makes the radial field at the surface significantly larger

Table 1 Surface magnetic field structures. A selection of the low-degree (ℓ) axisymmetric ($m = 0$) Gauss coefficients (in units of gauss) for the magnetic fields of Jupiter (Connerney et al. 1998), Saturn (Giampieri and Dougherty 2004) and the simulation by Glatzmaier (2005) (averaged in time). The sign of the axial dipole (g_1^0) defines the dipole polarity

Gauss coefficients			
ℓ	Jupiter g_ℓ^0	Saturn g_ℓ^0	Simulation g_ℓ^0
1	4.205	0.212	-2.770
2	-0.051	0.016	-1.041
3	-0.016	0.028	0.715
4	-0.168		-1.058

at high latitudes, as seen in Fig. 8. Also seen is the banded pattern of the radial component of the field at the surface, related to the banded pattern of the angular velocity.

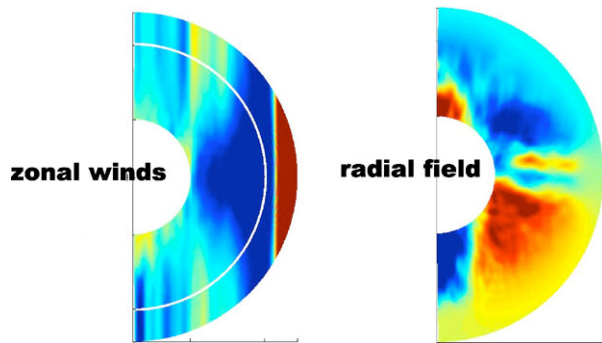
The simulation's dipole moment is $1.1 \times 10^{20} \text{ Tm}^3$, somewhat less than Jupiter's ($1.5 \times 10^{20} \text{ Tm}^3$) and larger than Saturn's ($4.2 \times 10^{18} \text{ Tm}^3$). More detailed structure of the magnetic field at and beyond the surface is usually described in terms of Gauss coefficients in a spherical harmonic expansion (e.g., Connerney et al. 1998). Table 1 lists a few of the lowest degree, ℓ , coefficients (i.e., largest scales) from fits to observations of the fields of Jupiter and Saturn and from the snapshot of the simulated field illustrated in Fig. 8. Better observations are needed to describe the planetary fields beyond degree 4 (see the paper by Dougherty and Russell in this issue); the computer simulation, in comparison, updates over 130,000 Gauss coefficients every numerical time step. Only the axisymmetric coefficients ($m = 0$) are listed here since the non-axisymmetric coefficients depend on the choice of the longitude zero and are more time dependent. However, it is seen that even the first four axisymmetric coefficients for the simulation do not agree with those for either planet, other than being of the same order of magnitude and having an axial dipole (g_1^0) that dominates. Note that its sign merely reflects the dipole polarity, which for the simulation is currently opposite of the present polarities for Jupiter and Saturn. The real problem is that many more than four degrees are needed to well describe even the axisymmetric part of the radial surface field vs latitude; the plot of this requires Gauss coefficients up to at least degree 15 before the high-latitude peaks become prominent as they are in Fig. 8. For example, the degree 9 coefficient is -1.087 gauss.

Future missions to Jupiter and Saturn that orbit much closer to their surfaces will provide more accurate estimates of higher degree magnetic structure and might detect a banded magnetic field structure as this simulation predicts. Gravity measurements in such missions could also test the banded cylindrical pattern of differential rotation deep below the surface (Hubbard 1990).

Since the amplitudes of the simulated zonal wind and magnetic field at the surface are somewhat similar to those of Jupiter and Saturn, it is instructive to check if the amplitudes and 3D geometrical configurations of the flows and fields well below the surface satisfy the constraint in (6) regarding the total rate of entropy production due to ohmic heating. Although time dependent, in general this constraint is satisfied in this simulation because the amplitude of the non-axisymmetric flow decreases with depth and because of the tendency for the field to satisfy Ferraro's iso-rotation law (Ferraro 1937; Glatzmaier 2008).

However, the spatial resolution of this simulation is not sufficient to capture small scale eddies and vortices near the surface. Actually, no deep convection simulation has yet even

Fig. 9 Snapshots of a Boussinesq simulation of a gas giant dynamo. *Left:* Zonally-averaged longitudinal velocity in the meridian plane. *Reds* are prograde; *blues* are retrograde. *Right:* Zonally-averaged radial magnetic field in the meridian plane. *Reds* are outward; *blues* are inward. (Heimpel and Gomez Perez 2008)



produced a large vortex at the surface like the “Great Red Spot”. This may require a representation of radiative transfer and moist convection near the surface, as is done in GCMs.

Another gas giant dynamo model has recently been developed by Heimpel and Gomez Perez (2008) based on their Boussinesq deep-convection model. In their model the convection zone represents the outer two-thirds in radius of the planet. Although density stratification is still neglected, this model has a prescribed electrical conductivity that increases exponentially by three orders of magnitude from the surface, R , down to radius $0.8 R$. Their electrical conductivity is constant in the highly-conducting metallic-hydrogen region below this radius. An intense magnetic field is maintained in this inner metallic region where the resulting Lorentz forces suppress the zonal wind amplitude (Fig. 9). The dominant feature in the outer low-conductivity region is a strong prograde equatorial jet. The magnetic field at the surface of their simulation is dominantly dipolar and much weaker than the field in the deep interior below $0.8 R$.

This simulation nicely demonstrates how an intense magnetic field can inhibit differential rotation. However, the field in the deep interior may be too intense because the convective flows there have amplitudes similar to those near the surface due to the model’s lack of density stratification.

Dynamo models have also been used to investigate the axisymmetry of Saturn’s magnetic field. Although Jupiter’s (and Earth’s) magnetic fields are dipole dominated, they still contain some observable amount of non-axisymmetry. For example the dipole tilts (ratio of equatorial dipole to axial dipole) for Earth and Jupiter are approximately 10 degrees (Stevenson 1983). In contrast, Saturn observations by Pioneer 11, Voyager I, II and Cassini obtain dipole tilts of < 0.1 –1 degrees and a similar lack of non-axisymmetry in the higher moments (Acuna and Ness 1980; Ness et al. 1981; Acuna et al. 1981, 1983; Smith et al. 1980; Davis and Smith 1990; Giampieri and Dougherty 2004). This almost perfect axisymmetry seems to contradict Cowling’s theorem (Cowling 1933) which states that a dynamo cannot maintain a purely axisymmetric field. However, Cowling’s theorem applies to the dynamo source region, so there is no contradiction if some mechanism can be found that axisymmetrizes the observed field outside the planet.

Stevenson (1980, 1982, 1983) suggested that a helium rain-out layer in Saturn could produce such a mechanism. At conditions in Saturn’s interior where hydrogen attains a significant conductivity, helium becomes immiscible in hydrogen and would therefore rain-out of the hydrogen. This would result in a thin stably-stratified layer surrounding the deep dynamo region. Stevenson proposed that differential rotation in this layer due to thermal winds could shear out the non-axisymmetry in the field. In Stevenson’s model, the thermal winds result because of pole to equator temperature differences at Saturn’s surface due to

solar insolation. Kinematic dynamo models have investigated the axisymmetrizing effects of stably-stratified layers surrounding the dynamo (Love 2000; Schubert et al. 2004). They found that flows in surrounding stable layers do not necessarily act to axisymmetrize the field. Depending on the interior field morphology and on the geometry of the stable layer zonal flows, a variety of field symmetries were produced.

Dynamic dynamo models have also investigated the effect of surrounding stable layers in an effort to explain Saturn. Christensen and Wicht (2008) found that with a thick stable layer, a highly axisymmetric field can result for certain parameter values. The average dipole tilt in their model is 1.5 degrees. However, their models work with a much thicker stable layer (~ 0.4 core radii) than the thin helium-rain out layer initially proposed. Thin stably-stratified layers have also been investigated by Stanley and Mohammadi (2008). These models demonstrated that coupling between the stable and unstable layers can act to destabilize the dynamo and result in more non-axisymmetry. However, these models do not drive flows in the stable layer via thermal winds the way Stevenson envisioned.

A recent model by Stanley (2008) employs an outer thermal boundary condition on the dynamo model to mimic the effect of laterally varying solar insolation, or alternatively, the thermal perturbations naturally produced by convection in Saturn's non-metallic outer layers (Aurnou et al. 2008). They find that the surface magnetic fields can be axisymmetrized through these zonal flows, but only when the boundary thermal perturbations result in thermal winds matching the sign and morphology of those already occurring in the deeper interior. The necessary profile to produce axisymmetrization is the expected profile for solar insolation or atmospheric convection scenarios. This suggests that Stevenson's mechanism may explain the axisymmetrization of Saturn's magnetic field. Of course, since these models employ the Boussinesq approximation and do not model the outer layers of Saturn, they are intended more to study the specific mechanism for Saturn axisymmetrization rather than produce a complete model of Saturn's interior flows. In addition, vigorous convection may easily overshoot through a thin stably-stratified layer, both from below and from above, completely dominating any thermal wind driving by solar insolation at the surface.

An important question regarding the axisymmetrization of Saturn's magnetic field and regarding the dynamo mechanism in general for giant planets is how deep do the observed zonal winds extend below the surface, i.e., what is the differential rotation in radius and latitude. Liu et al. (2008) attempt to answer this question by doing a steady-state, axisymmetric, kinematic scale-analysis. By estimating the amount of electric current that would be generated within the interior with their prescribed differential rotation shearing their prescribed internal magnetic field and using their estimate of the depth-dependent electrical conductivity they get an estimate of the total amount of ohmic heating as a function of the depth of the differential rotation. Assuming that this ohmic heating cannot exceed the observed luminosity, they predict that the zonal winds extend no deeper than 0.96 of Jupiter's radius and 0.85 of Saturn's radius.

This is a bold attempt to answer a difficult question, especially without the aid of a 3D self-consistent convective dynamo simulation. However, their analysis has several uncertainties (Glatzmaier 2008; Jones and Kuzanyan 2009). As shown by Backus (1975), Hewitt et al. (1975), the total ohmic heating can exceed the luminosity because the bulk of the dissipation occurs at a much higher temperature than the surface temperature. Also, as shown by Ferraro (1937) for the conditions assumed by Liu et al. (2008), if the internal poloidal field is everywhere parallel to surfaces of constant angular velocity there would be no electric current generated and therefore no ohmic heating produced. Of course, some current needs to be generated to maintain a global magnetic field and so the dynamo mechanism is intimately connected with the differential rotation below the surface. How well the field obeys

the Ferraro iso-rotation law and allows deep-seated zonal winds in gas giants is still an open question.

3.4.2 *Ice Giants*

The magnetic fields of Uranus and Neptune are non-axially, non-dipolar dominated (see papers by Dougherty and Russell and by Fortney in this issue). It turns out that generating axial-dipolar dominated dynamo models is relatively easy when working in an Earth-like thick shell geometry with standard boundary conditions and driving forces. Even observations suggest that axial-dipolar dominated fields are the norm since both Earth and Jupiter have similar magnetic field morphologies although vastly different interior structure and composition. Explaining the ice giants' anomalous fields has therefore resided in understanding what could be different inside these planets to result in such strange magnetic fields.

Kinematic dynamo models investigating field symmetries show that axial dipolar, axial quadrupolar, and equatorial dipolar magnetic fields can result from very similar flows, suggesting that it may not be difficult to generate non-axial-dipole dominated fields (Gubbins et al. 2000). Indeed, although the majority of Earth-like geometry dynamo models produce axially dipolar dominated fields, non-dipolar, non-axisymmetric dynamo models have been found (Grote et al. 1999, 2000; Grote and Busse 2000; Ishihara and Kida 2000; Aubert and Wicht 2004). These solutions are found in isolated regions of parameter space and it remains unknown whether these solutions would exist in the planetary parameter regime (although one has to admit that this is also the case for the axial-dipole dominated dynamo models). However, there are two fundamental issues in using these models to explain Uranus' and Neptune's fields: (i) These non-axial-dipolar dominated dynamos produce much simpler fields than observed in Uranus and Neptune. They are dominated by a specific component of the large scale field whereas Uranus and Neptune have significant power in several modes (e.g. dipole, quadrupole, octupole, axisymmetric and non-axisymmetric). (ii) These models do not match the structure of the ice giant interiors determined from their low heat flows (Podolak et al. 1991; Hubbard et al. 1995). It is therefore unclear as to whether these simpler models can explain Uranus' and Neptune's fields. However, they are certainly important in understanding mechanisms of non-dipolar non-axial field generation.

Kutzner and Christensen (2002) found that non-dipolarity increases with Rayleigh number, suggesting that one could explain Uranus and Neptune by saying they convect more vigorously than the other planets. However, based on observations of Uranus' and Neptune's low heat flows, it seems unlikely that the ice giants are more supercritical than the gas giants.

Uranus' and Neptune's low heat flows resulted in an early proposition to explain their magnetic fields. Hubbard et al. (1995) demonstrated that the observed heat flux is inconsistent with whole-planet convection. They showed that the heat flows imply that only the outer 0.4 Uranus radii and 0.6 Neptune radii of the planets are convectively unstable. They suggest that the stably-stratified interior regions can explain the low heat flows and possibly also the anomalous magnetic fields since this stratification results in a thin-shell dynamo geometry. The stratification is due to compositional gradients in the interiors of the planets which are not unreasonable considering the composition and thermal evolution of the ice giants.

Stanley and Bloxham (2004, 2006) investigated whether dynamos operating in thin layers surrounding stably-stratified interiors could produce Uranus and Neptune like fields. They found that non-dipolar, non-axisymmetric fields resulted with similar surface power spectra to the observations from these planets. This is due to the influence of the stably stratified interior on the stability of the dipole component in these models. Thin shell models surrounding

insulating solid interiors, conducting solid interiors and stably-stratified fluid interiors were investigated. It was found that, although the fluid flows in these models are relatively similar in morphology and intensity, insulating solid inner core models and stably-stratified inner region models produced magnetic fields with a very different morphology than the conducting solid inner core models. In the conducting solid inner core models, the anchoring effect due to the inner core on magnetic field lines stabilized the dynamo producing a strong dipolar field. When the electrical conductivity of the inner core was removed, this anchoring effect was reduced, and in combination with the thinner shell geometry, resulted in smaller scale (non-dipolar, non-axisymmetric) fields that reversed continuously. Models with thin shells surrounding stably-stratified interiors produced similar fields to the insulating solid inner core models because the fluid inner core can mimic an insulating solid core in its response to electromagnetic stress. The stably-stratified interior loses its anchoring influence because the magnetic fields can differentially move the fluid, whereas they cannot do so in a solid conducting interior.

These dynamo models only considered the deep regions of the planet where the pressures are high enough such that the electrical conductivity is substantial enough to drive a dynamo. The outer layers of the planet are not modeled. Models by Gomez-Perez and Heimpel (2007) instead consider the outer regions of the planets as well by incorporating a radially variable electrical conductivity. They find that the deeper regions of the planets which have the larger conductivity have much weaker zonal flows than the outer, relatively more insulating layers. The higher magnetic diffusivities in these models, combined with the surrounding zonal flows, can result in non-dipolar, non-axisymmetric fields. Similar to the Stanley and Bloxham (2004) models, these models produce complex fields with similar power spectra as those of Uranus and Neptune observations. However, they do not adhere to the interior geometry constrained by the heat flow observations.

3.5 Extrasolar Planet Models

More than 300 extrasolar giant planets have been detected during the past decade using Doppler measurements of the periodic orbital velocities of their sun-like parent stars. A small number have also been detected using photometry during their transits in front of and behind their parent stars. Extrasolar terrestrial planets, because of their much smaller mass, have been much more difficult to detect.

The extrasolar giants that have been discovered have small orbits because of an observational selection effect due to the correspondingly short orbital periods. Having orbital radii as small as 0.05 AU, compared to Jupiter's 5 AU orbital radius, makes the incident stellar radiation four orders of magnitude greater than that received by Jupiter from our sun. The small orbital radii also mean large tidal effects; so it is assumed that the rotation and orbital periods of these planets are nearly synchronous (e.g., Goldreich and Soter 1966). That is, one hemisphere is always facing the parent star and the other is always hidden from it. This external heating, especially on the dayside, likely produces a very stable thermal stratification down to much greater pressures in these "Hot Jupiters" than the roughly 1 bar pressure level that marks the top of the convection zone in our solar system giants. This extreme day-side heating and nightside cooling must also drive strong atmospheric circulations. What structure these winds have and how deep they extend have been key questions on which several modeling groups have attempted to shed light.

Many modeling studies of the non-magnetic surface dynamics on Hot Jupiters have come from the atmospheric climate modeling community. Like the GCMs for solar system giants, these models completely neglect convection in the deep interior and the zonal winds it maintains. For a nice review of these see Showman et al. (2007).

These models predict wind speeds up to 10^5 m/s and atmospheric temperatures up to 10^4 K, which means that in some regions these winds can be supersonic. GCMs do not simulate supersonic flows; nor do anelastic models. This problem requires a model that solves the fully-compressible radiative-hydrodynamic equations. The price one pays is that the numerical time step needs to be much smaller in order to resolve sound waves. Dobbs-Dixon and Lin (2008) have used such a model to study 3D winds in a Hot Jupiter. This model simulates roughly the outer 8% in radius of the planet and does not make the shallow-water simplifications employed in GCMs. Their model treats the radiation transfer using a flux-limited method that smoothly varies from the diffusion limit (for an optically thick region) to the streaming limit (for an optically thin region). The simulated winds reach a Mach number of 2.7. The zonal wind pattern has a broad prograde equatorial jet and mid-latitude retrograde jets. They argue how important it is for this problem to solve the full 3D momentum equation and employ a self-consistent treatment of the radiation transfer. However, they do not address the dynamics of the deep interior.

Evonuk and Glatzmaier (2009) have developed an anelastic model to study convection and zonal winds of the deep interior of an extrasolar gas giant, assuming a negligible magnetic field. The model is a fully-convective density-stratified rotating fluid *sphere*; but the model's top boundary is placed below the shallow weather layer. Vigorous convection is driven throughout the model planet by a heat source in the central region meant to represent the heat generated by the slow contraction of the planet. When the planetary rotation is relatively weak compared to buoyancy, the preferred mode of convection is a dipolar flow through the center of the planet; a greater rotational influence results in strong zonal flows that extend deep into the interior. The winds at the model's surface have a broad prograde equatorial jet and mid-latitude retrograde jets.

What have not yet been studied are the types of magnetic fields that could be generated in extrasolar gas giants. The proximity of Hot Jupiters to their parent stars suggests that the outer atmospheres of these planets are partially ionized and therefore electrically conducting. The type of dynamos that operate in these supersonic surface flows is a fascinating unstudied problem. Ideally, for Hot Jupiters, the dynamos of both the parent star and the gas giant should be simulated simultaneously with robust treatments of the gravitational, radiation and magnetic interactions.

3.6 Future Model Improvements

Future convective dynamo models of giant planets should include more realistic radial stratifications of density and electrical conductivity. They should solve the full momentum equation, as done in deep convection models, and should include radiative transfer and moist convection using schemes near the surface that are at least as self-consistent and sophisticated as those employed in GCMs of the Earth's atmosphere. Higher spatial resolution will also be needed so viscosity and thermal conductivity can be reduced and more strongly turbulent convection can be simulated.

The velocity boundary conditions prescribed in these models also need to be improved. The top boundary should not continue to be a fixed impermeable boundary, which artificially forces radial flow into horizontal flow. The vertical coordinate could instead be the column mass, as in one dimensional planetary evolutionary models, or some variation of pressure, as in GCMs. Alternatively, if one wishes to continue using radius as the vertical coordinate, permeable "free surface" boundaries should be employed within a stratosphere.

The treatment of the very deep interior should also be improved. Some extrasolar giant planets (and possibly also Jupiter) likely have no solid core or even a stably-stratified fluid

core at some time in their evolution. Models of these planets require a full sphere instead of a spherical shell. As discussed above, preliminary full-sphere rotating, stratified, convection calculations have been produced (Evonuk and Glatzmaier 2009); however, these need to be run as a dynamo to see how the field and flow interact in the deep interior constrained by the rate of entropy production by ohmic heating.

Other complications that need to be addressed in simulation studies of giant planets are the hydrogen phase transition and helium settling (Stevenson and Salpeter 1977; Guillot et al. 2004), double diffusive convection (e.g., Stellmach et al. 2009) and tidal effects and inertial modes (e.g., Guillot et al. 2004; Tilgner 2007).

4 Satellite Dynamos

At least two moons in our solar system have evidence for dynamo action sometime during their history. Observations from the Galileo mission demonstrated that Ganymede has an intrinsic field most likely due to an active dynamo (Kivelson et al. 1996). Data from various missions showed that Earth's Moon, on the other hand, possesses localized crustal magnetic fields which may be evidence of a past dynamo (Fuller and Cisowski 1987; Halekas et al. 2001). Further information on lunar magnetism comes from the magnetization of Apollo samples allowing constraints to be placed on the timing of the lunar dynamo (Cisowski et al. 1983; Garrick-Bethel et al. 2009). These two bodies maintain some of the most intriguing questions in planetary magnetic fields.

For Ganymede, the Galileo mission measured a dipole moment, but no information on the higher multipoles is available. The data can be modeled relatively well by an appropriately scaled Earth-dynamo model. However, the question remains as to how a small body like Ganymede can maintain a present-day fluid outer core with strong convection (although perhaps this is not as surprising in light of the fact that Mercury does as well). The presence of sulfur in Ganymede's core is employed to explain this, and the possibility that the driving force for Ganymede is freezing of iron snow below the CMB (Hauck et al. 2006) suggest that there may be work for dynamo modelers yet. In addition, the orbital resonances of the four Galilean satellites may provide alternative driving mechanisms for Ganymede in its past, as well as an additional heat source maintaining Ganymede's fluid outer core. A mean-field model for Ganymede investigated the effects of Jupiter's magnetic field in aiding the generation of Ganymede's field by providing a source field for the convective motions to interact with Sarson et al. (1997). They found that although Jupiter's seed magnetic field is not required to maintain Ganymede's dynamo, it may influence the polarity of the resulting field.

If the Moon's remanent magnetic field is the result of rocks cooling in the presence of an ancient dynamo (rather than due to impact magnetization, Hood and Artemieva 2008), then it must contain a metallic core; a piece of information current interior models cannot verify. Thermal evolution models for the Moon suggest that it can maintain a short-lived dynamo early in its history, or slightly later in its history if the core is insulated early on by a radioactive thermal blanket (Stegman et al. 2003). Impact magnetization and demagnetization have likely played a role in shaping the morphology of the crustal field, but not enough information is available to constrain the dynamo generated field from the crustal remanent fields, and hence no dynamo models. However, one aspect of the Moon which dynamo modelers should investigate is the importance of mechanical stirring due to the stronger tidal forces in the past.

5 Conclusions

Since magnetic fields are generated in a planet's deep interior and extend beyond the surface where they are observable, magnetic fields can act as important probes of planetary interior structure and dynamics. Planetary dynamo models therefore, not only investigate the magnetic field generation process, but also tell us about regions of the planet difficult to study with other means. Current planetary dynamo models have opened a window into planetary cores, providing insights into core fluid flows, convective stability and thermal evolution. However, much work is still needed before the planetary dynamo process is fully understood and we can take full advantage of the implications of planetary magnetic field observations.

The main improvements needed are in numerical modeling methods and computational power and better observational and experimental data on magnetic fields, interior structure and dynamics. Current and near-future planetary missions such as MESSENGER, Bepi-Colombo, Juno and Grail will hopefully provide us with new constraints on the planetary dynamo process.

Acknowledgement G.G. thanks NASA for support under grants NNG05GG69G and NNX09AD89G. S.S. thanks NSERC for support under the Discovery Grants program.

References

- M.H. Acuna, N. Ness, The magnetic field of Saturn: Pioneer 11 observations. *Science* **207**, 444–446 (1980)
- M.H. Acuna, J. Connerney, N. Ness, Topology of Saturn's main magnetic field. *Nature* **292**, 721–726 (1981)
- M.H. Acuna, J. Connerney, N. Ness, The Z_3 zonal harmonic model of Saturn's magnetic field: Analyses and implications. *J. Geophys. Res.* **88**, 8771–8778 (1983)
- M.H. Acuna et al., Global distribution of crustal magnetization discovered by the Mars Global Surveyor MAG/ER experiment. *Science* **284**, 790–793 (1999)
- O. Aharonson, M. Zuber, S. Solomon, Crustal remanence in an internally magnetized non-uniform shell: a possible source for Mercury's magnetic field? *Earth Planet. Sci. Lett.* **218**, 261–268 (2004)
- M. Allison, A similarity model for the windy jovian thermocline. *Planet. Space Sci.* **48**, 753–774 (2000)
- B. Anderson et al., The structure of Mercury's magnetic field from MESSENGER's first flyby. *Science* **321**, 82–85 (2008)
- J. Andrews-Hanna, M. Zuber, W. Banerdt, The Borealis basin and the origin of the martian crustal dichotomy. *Nature* **453**, 1212–1215 (2008)
- J. Arkani-Hamed, B. Seyed-Mahmoud, K.D. Aldridge, R.E. Baker, Tidal excitation of elliptical instability in the Martian core: Possible mechanism for generating the core dynamo. *J. Geophys. Res.* **113** (2008). doi:[10.1029/2007JE002982](https://doi.org/10.1029/2007JE002982)
- D.H. Atkinson, J.B. Pollack, A. Seiff, The Galileo Probe Doppler Wind Experiment: measurement of the deep zonal winds on Jupiter. *J. Geophys. Res.* **103**, 22911–22928 (1998)
- J. Aubert, J. Wicht, Axial vs. equatorial dipolar dynamo models with implications for planetary magnetic fields. *Earth Planet. Sci. Lett.* **221**, 409–419 (2004)
- J. Aubert, D. Brito, H.-C. Nataf, P. Cardin, J.-P. Masson, A systematic experimental study of rapidly rotating spherical convection in water and liquid gallium. *Phys. Earth Planet. Inter.* **128**, 51–74 (2001)
- J.M. Aurnou, Planetary core dynamics and convective heat transfer scaling. *Geophys. Astrophys. Fluid Dyn.* **101**, 327–345 (2007)
- J.M. Aurnou, M. Heimpel, J. Wicht, The effects of vigorous mixing in a convective model of zonal flow on the ice giants. *Icarus* **190**, 110–126 (2007)
- J. Aurnou, M. Heimpel, L. Allen, E. King, J. Wicht, Convective heat transfer and the pattern of thermal emission on the gas giants. *Geophys. J. Int.* **173**, 793–801 (2008)
- G.E. Backus, Gross thermodynamics of heat engines in the deep interior of the Earth. *Proc. Natl. Acad. Sci. Wash.* **72**, 1555–1558 (1975)
- P. Bodenheimer, G. Laughlin, D.N.C. Lin, On the radii of extrasolar giant planets. *Astrophys. J.* **592**, 555–563 (2003)

- D. Breuer, T. Spohn, Early plate tectonics versus single-plate tectonics on Mars: Evidence from magnetic field history and crust evolution. *J. Geophys. Res.* **108** (2003). doi:[10.1029/2002JE001999](https://doi.org/10.1029/2002JE001999)
- D. Breuer, D.A. Yuen, T. Spohn, S. Zhang, Three dimensional models of Martian mantle convection with phase transitions. *Geophys. Res. Lett.* **25**, 229–232 (1998)
- F.H. Busse, A model of mean zonal flows in the major planets. *Geophys. Astrophys. Fluid Dyn.* **23**, 153–174 (1983)
- F.H. Busse, Convective flows in rapidly rotating spheres and their dynamo action. *Phys. Fluids* **14**, 1301–1314 (2002)
- F.H. Busse, C.R. Carrigan, Laboratory simulation of thermal convection in rotating planets and stars. *Science* **191**, 81–83 (1976)
- B. Chen, J. Li, S. Hauck, Non-ideal liquidus curve in the Fe-S system and Mercury's snowing core. *Geophys. Res. Lett.* **35** (2008). doi:[10.1029/2008GL033311](https://doi.org/10.1029/2008GL033311)
- S. Childress, A. Soward, Convection-driven hydromagnetic dynamo. *Phys. Rev. Lett.* **29**, 837–839 (1972)
- J.Y.-K. Cho, L.M. Polvani, The morphogenesis of bands and zonal winds in the atmospheres on the giant outer planets. *Science* **273**, 335–337 (1996)
- U.R. Christensen, Zonal flow driven by strongly supercritical convection in rotating spherical shells. *J. Fluid Mech.* **470**, 115–133 (2002)
- U. Christensen, A deep dynamo generating Mercury's magnetic field. *Nature* **444**, 1056–1058 (2006)
- U. Christensen, J. Wicht, Models of magnetic field generation in partly stable planetary cores: Applications to Mercury and Saturn. *Icarus* **196**, 16–34 (2008)
- S. Cisowski, D. Collinson, S. Runcorn, A. Stephenson, M. Fuller, A review of lunar paleointensity data and implications for the origin of lunar magnetism. *J. Geophys. Res.* **88**, 691–704 (1983)
- J. Connerney, Magnetic fields of the outer planets. *J. Geophys. Res.* **98**, 18659–18679 (1993)
- J. Connerney, M.H. Acuna, N.F. Ness, T. Satoh, New models of Jupiter's magnetic field constrained by the Io flux tube footprint. *J. Geophys. Res.* **103**, 11929–11939 (1998)
- T. Cowling, The magnetic field of sunspots. *Mon. Not. R. Astron. Soc.* **94**, 39–48 (1933)
- L. Davis, E. Smith, A model of Saturn's magnetic field based on all available data. *J. Geophys. Res.* **95**, 15257–15261 (1990)
- I. Dobbs-Dixon, D.N.C. Lin, Atmospheric dynamics of short-period extrasolar gas giant planets I. Dependence of nightside temperature on opacity. *Astrophys. J.* **673**, 513–548 (2008)
- E. Dormy, J.-P. Valet, V. Courtillot, Numerical models of the geodynamo and observational constraints. *Geochem. Geophys. Geosyst.* **1** (2000), paper 2000GC000062
- T.E. Dowling, Dynamics of Jovian atmospheres. *Ann. Rev. Fluid Mech.* **27**, 293–334 (1995)
- L. Elkins-Tanton, E. Parmentier, P. Hess, Magma ocean fractional crystallization and cumulate overturn in terrestrial planets: Implications for Mars. *Meteorit. Planet. Sci.* **38**, 1753–1771 (2003)
- L. Elkins-Tanton, S. Zaranek, E. Parmentier, P. Hess, Early magnetic field and magmatic activity on Mars from magma ocean cumulate overturn. *Earth Planet. Sci. Lett.* **236**, 1–12 (2005)
- M. Evonuk, G.A. Glatzmaier, Thermal convection in a 3D rotating density-stratified giant planet without a core. *Geophys. J. Int.* (2009, under review)
- V.C.A. Ferraro, The nonuniform rotation of the Sun and its magnetic field. *Mon. Not. R. Astron. Soc.* **97**, 458–472 (1937)
- H. Frey, R. Shultz, Large impact basins and the mega-impact origin for the crustal dichotomy on Mars. *Geophys. Res. Lett.* **15**, 229–232 (1988)
- M. Fuller, S. Cisowski, Lunar paleomagnetism, in *Geomagnetism*, vol. 2, ed. by J. Jacobs (Academic Press, San Diego, 1987), pp. 307–456
- I. Garrick-Bethel, B. Weiss, D. Shuster, J. Buz, Early lunar magnetism. *Science* **323**, 356–359 (2009)
- G. Giampieri, A. Balogh, Mercury's thermoelectric dynamo model revisited. *Planet. Space Sci.* **50**, 757–762 (2002)
- G. Giampieri, M. Dougherty, Rotation rate of Saturn's interior from magnetic field observations. *Geophys. Res. Lett.* **31** (2004). doi:[10.1029/2004GL020194](https://doi.org/10.1029/2004GL020194)
- G. Giampieri, M.K. Dougherty, E.J. Smith, C.T. Russell, A regular period for Saturn's magnetic field that may track its internal rotation. *Nature* **441**, 62–64 (2006)
- P.A. Gilman, J. Miller, Dynamically consistent nonlinear dynamos driven by convection in a rotating spherical shell. *Astrophys. J. Suppl.* **46**, 211–238 (1981)
- K.H. Glassmeier, H.U. Auster, U. Motschmann, A feedback dynamo generating Mercury's magnetic field. *Geophys. Res. Lett.* **34** (2007a). doi:[10.1029/2007GL031662](https://doi.org/10.1029/2007GL031662)
- K.H. Glassmeier et al., Electromagnetic induction effects and dynamo action in the Hermean system. *Space Science Rev.* **132**, 511–527 (2007b)
- G.A. Glatzmaier, Numerical simulations of stellar convective dynamos I. The model and method. *J. Comput. Phys.* **55**, 461–484 (1984)

- G.A. Glatzmaier, Geodynamo simulations—How realistic are they? *Ann. Rev. Earth Planet. Sci.* **30**, 237–257 (2002)
- G.A. Glatzmaier, A saturnian dynamo simulation. American Geophysical Union Fall Meeting 2005, San Francisco, CA (2005)
- G.A. Glatzmaier, A note on Constraints on deep-seated zonal winds inside Jupiter and Saturn. *Icarus* **196**, 665–666 (2008)
- G.A. Glatzmaier, P.A. Gilman, Compressible convection in a rotating spherical shell. III. Analytic model for compressible vorticity waves. *Astrophys. J. Suppl.* **45**, 381–388 (1981)
- G.A. Glatzmaier, P.A. Gilman, Compressible convection in a rotating spherical shell. V. Induced differential rotation and meridional circulation. *Astrophys. J.* **256**, 316–330 (1982)
- G.A. Glatzmaier, R.S. Coe, L. Hongre, P.H. Roberts, The role of the Earth's mantle in controlling the frequency of geomagnetic reversals. *Nature* **401**, 885–890 (1999)
- G.A. Glatzmaier, M. Evonuk, T.M. Rogers, Differential rotation in giant planets maintained by density-stratified turbulent convection. *Geophys. Astrophys. Fluid Dyn.* **103**, 31–51 (2009)
- P. Goldreich, S. Soter, Q in the solar system. *Icarus* **5**, 375–389 (1966)
- N. Gomez-Perez, M. Heimpel, Numerical models of zonal flow dynamos: an application to the ice giants. *Geophys. Astrophys. Fluid Dyn.* **101**, 371–388 (2007)
- J. Grosser, K.H. Glassmeier, A. Stadelmann, Induced magnetic field effects at planet Mercury. *Planet. Space Sci.* **52**, 1251–1260 (2004)
- E. Grote, F. Busse, Hemispherical dynamos generated by convection in rotating spherical shells. *Phys. Rev. E* **62**, 4457–4460 (2000)
- E. Grote, F. Busse, A. Tilgner, Convection-driven quadrupolar dynamos in rotating spherical shells. *Phys. Rev. E* **60**, 5025–5028 (1999)
- E. Grote, F. Busse, A. Tilgner, Regular and chaotic spherical dynamos. *Phys. Earth Planet. Int.* **117**, 259–272 (2000)
- D. Gubbins, C. Barber, S. Gibbons, J. Love, Kinematic dynamo action in a sphere II. Symmetry selection. *Proc. R. Soc. Lond. A* **456**, 1669–1683 (2000)
- T. Guillot, A comparison of the interiors of Jupiter and Saturn. *Planet. Space Sci.* **47**, 1183–1200 (1999)
- T. Guillot, The interiors of giant planets: models and outstanding questions. *Ann. Rev. Earth Planet. Sci.* **33**, 493–530 (2005)
- T. Guillot, D.J. Stevenson, W.B. Hubbard, D. Saumon, The interior of Jupiter, in *Jupiter: The Planet, Satellites and Magnetosphere*, ed. by F. Bagenal, T. Dowling, W. McKinnon (Cambridge Univ. Press, Cambridge, 2004)
- J. Halekas et al., Mapping of crustal magnetic anomalies on the lunar near side by the Lunar Prospector electron reflectometer. *J. Geophys. Res.* **106**, 27841–27852 (2001)
- H.B. Hammel, I. de Pater, S. Gibbard, G.W. Lockwood, K. Rages, Uranus in 2003: zonal winds, banded structure, and discrete features. *Icarus* **175**, 534–545 (2005)
- C.J. Hansen, S.D. Kawaler, *Stellar Interiors: Physical Principles, Structure, and Evolution. Astronomy and Astrophysics Library* (Springer, Berlin, 1994)
- J.E. Hart, G.A. Glatzmaier, J. Toomre, Spacelaboratory and numerical simulations of thermal convection in a rotating hemispherical shell with radial gravity. *J. Fluid Mech.* **173**, 519–544 (1986)
- H. Harder, Phase transitions and the three-dimensional planform of thermal convection in the Martian mantle. *J. Geophys. Res.* **103**, 16775–16797 (1998)
- S. Hauck, J. Aurnou, A. Dombard, Sulfur's impact on core evolution and magnetic field generation on Ganymede. *J. Geophys. Res.* **111** (2006). doi:10.1029/2005JE002557
- M. Heimpel, N. Gomez-Perez, Numerical models of the transition from zonal flow to dynamo action in Jupiter and Saturn. American Geophysical Union Fall Meeting 2008, P11B-1276, San Francisco, CA (2008)
- M. Heimpel, J. Aurnou, F. Al-Shamali, N. Gomez-Perez, A numerical study of dynamo action as a function of spherical shell geometry. *Earth Planet. Sci. Lett.* **236**, 542–557 (2005a)
- M. Heimpel, J. Aurnou, J. Wicht, Simulation of equatorial and high-latitude jets on Jupiter in a deep convection model. *Nature* **438**, 193–196 (2005b)
- J.M. Hewitt, D.P. McKenzie, N.O. Weiss, Dissipative heating in convective flows. *J. Fluid Mech.* **68**, 721–738 (1975)
- D. Heyner et al., Concerning the initial temporal evolution of a Hermean feedback dynamo. *Earth Planet. Sci. Lett.* (2009, submitted)
- L. Hood, N. Artemieva, Antipodal effects of lunar basin-forming impacts: Initial 3D simulations and comparisons with observations. *Icarus* **193**, 485–502 (2008)
- W.B. Hubbard, Gravitational signature of Jupiter's deep zonal flows. *Icarus* **137**, 357–359 (1990)
- W. Hubbard, M. Podolak, D. Stevenson, Interior of Neptune, in *Neptune and Triton*, ed. by D. Cruickshank (University of Arizona Press, Tucson, 1995), pp. 109–138

- N. Ishihara, S. Kida, Axial and equatorial magnetic dipoles generated in a rotating spherical shell. *J. Phys. Soc. Jpn.* **69**, 1582–1585 (2000)
- C.A. Jones, K.M. Kuzanyan, Compressible convection in the deep atmospheres of giant planets. *Icarus* (2009, in press)
- Y. Ke, V. Solomatov, Early transient superplumes and the origin of the Martian crustal dichotomy. *J. Geophys. Res.* **111** (2006). doi:[10.1029/2005JE002631](https://doi.org/10.1029/2005JE002631)
- M. Kivelson et al., Discovery of Ganymede's magnetic field by the Galileo spacecraft. *Nature* **384**, 537–541 (1996)
- M. Kono, P.H. Roberts, Recent geodynamo simulations and observations of the geomagnetic field. *Rev. Geophys.* **40**, 4–1–53 (2002)
- W. Kuang, W. Jiang, T. Wang, Sudden termination of Martian dynamo? Implications from subcritical dynamo simulations. *Geophys. Res. Lett.* **35** (2008). doi:[10.1029/2008GL034183](https://doi.org/10.1029/2008GL034183)
- C. Kutzner, U. Christensen, From stable dipolar towards reversing numerical dynamos. *Phys. Earth Planet. Int.* **131**, 29–45 (2002)
- Y. Lian, A.P. Showman, Generation of zonal jets by moist convection on the giant planets. *Icarus* (2009, under review)
- J. Liu, P.M. Goldreich, D.J. Stevenson, Constraints on deep-seated zonal winds inside Jupiter and Saturn. *Icarus* **196**, 506–517 (2008)
- J. Love, Dynamo action and the nearly axisymmetric magnetic field of Saturn. *Geophys. Res. Lett.* **27**, 2889–2892 (2000)
- J.B. Manneville, P. Olson, Banded convection in rotating fluid spheres and the circulation of the jovian atmosphere. *Icarus* **122**, 242–250 (1996)
- J. Margot, S. Peale, R. Jurgens, M. Slade, I. Holin, Large longitude libration of Mercury reveals a molten core. *Science* **316**, 710–714 (2007)
- M. Marinova, O. Aharonson, E. Asphaug, Mega-impact formation of the Mars hemispheric dichotomy. *Nature* **453**, 1216–1219 (2008)
- N. Ness, K. Behannon, R. Lepping, Y. Whang, Magnetic field of Mercury confirmed. *Science* **255**, 204–206 (1975)
- N. Ness, K. Behannon, R. Lepping, Y. Whang, Observations of Mercury's magnetic field. *Icarus* **28**, 479–488 (1976)
- N. Ness et al., Magnetic field studies by Voyager 1: Preliminary results at Saturn. *Science* **212**, 211–217 (1981)
- F. Nimmo, D. Stevenson, Influence of early plate tectonics on the thermal evolution and magnetic field of Mars. *J. Geophys. Res.* **105**, 11969–11979 (2000)
- F. Nimmo, S. Hart, D. Korycansky, C. Agnor, Implications of an impact origin for the martian hemispheric dichotomy. *Nature* **453**, 1220–1223 (2008)
- M. Podolak, W. Hubbard, D. Stevenson, Models of Uranus' interior and magnetic field, in *Uranus*, ed. by J. Bergstrahl, E. Minor, M. Matthews (University of Arizona Press, Tucson, 1991), pp. 29–61
- C.C. Porco, R.A. West, A. McEwen et al., Cassini imaging of Jupiter's atmosphere, satellites, and rings. *Science* **299**, 1541–1547 (2003)
- J. Proudman, On the motion of solids in a liquid possessing vorticity. *Proc. R. Soc. Lond. A* **92**, 408–424 (1916)
- P.B. Rhines, Waves and turbulence on a beta-plane. *J. Fluid Mech.* **69**, 417–443 (1975)
- J. Roberts, S. Zhong, Degree-1 convection in the Martian mantle and the origin of the hemispheric dichotomy. *J. Geophys. Res.* **111** (2006). doi:[10.1029/2005JE002668](https://doi.org/10.1029/2005JE002668)
- A. Sanchez-Lavega, S. Perez-Hoyos, J.F. Rojas, R. Hueso, R.G. French, A strong decrease in Saturn's equatorial jet at cloud level. *Nature* **423**, 623–625 (2002)
- G. Sarson, C. Jones, K. Zhang, G. Schubert, Magnetotconvection dynamos and the magnetic fields of Io and Ganymede. *Science* **276**, 1106–1108 (1997)
- G. Schubert, M. Ross, D. Stevenson, T. Spohn, Mercury's thermal history and the generation of its magnetic field, in *Mercury*, ed. by F. Vilas, C. Chapman, M. Matthews (University of Arizona Press, Tucson, 1988), pp. 429–460
- G. Schubert, K. Chan, X. Liao, K. Zhang, Planetary dynamos: Effects of electrically conducting flows overlying turbulent regions of magnetic field generation. *Icarus* **172**, 305–315 (2004)
- A.P. Showman, K. Menou, J.Y.-K. Cho, Atmospheric circulation of hot Jupiters: a review of current understanding, in *APS Conf. Ser.*, ed. by F. Rasio et al. (APS, San Francisco, 2007)
- E. Smith et al., Saturn's magnetic field and magnetosphere. *Science* **207**, 407–410 (1980)
- L. Srnka, Magnetic dipole moment of a spherical shell with TRM acquired in a field of internal origin. *Phys. Earth Planet. Int.* **11**, 184–190 (1976)
- S. Stanley, A dynamo model of Saturn's extremely axisymmetric internal magnetic field. *Eos Trans. AGU* **89**(23), Jt. Assem. Suppl., Abstract GP31A-02 (2008)

- S. Stanley, J. Bloxham, Convective-region geometry as the cause of Uranus' and Neptune's unusual magnetic fields. *Nature* **428**, 151–153 (2004)
- S. Stanley, J. Bloxham, Numerical dynamo models of Uranus' and Neptune's magnetic fields. *Icarus* **184**, 556–572 (2006)
- S. Stanley, A. Mohammadi, Effects of an outer thin stably stratified layer on planetary dynamos. *Phys. Earth Planet. Int.* **168**, 179–190 (2008)
- S. Stanley, J. Bloxham, W. Hutchison, M. Zuber, Thin shell dynamo models consistent with Mercury's weak observed magnetic field. *Earth Planet. Sci. Lett.* **234**, 27–38 (2005)
- S. Stanley, L. Elkins-Tanton, M. Zuber, E.M. Parmentier, Mars' paleomagnetic field as the result of a single-hemisphere dynamo. *Science* **321**, 1822–1825 (2008)
- S.V. Starchenko, C.A. Jones, Typical velocities and magnetic field strengths in planetary interiors. *Icarus* **157**, 426–435 (2002)
- D. Stegman, A. Hellinek, S. Zatman, J. Baumgardner, M. Richards, An early lunar core dynamo driven by thermochemical mantle convection. *Nature* **421**, 143–146 (2003)
- S. Stellmach, P. Garaud, A. Traxler, N. Brummell, T. Radko, 3D simulations of layer formation by compositionally driven double diffusive convection. *Science* (2009, under review)
- A. Stephenson, Crustal remanence and the magnetic moment of Mercury. *Earth Planet. Sci. Lett.* **28**, 454–458 (1975)
- D. Stevenson, Saturn's luminosity and magnetism. *Science* **208**, 746–748 (1980)
- D. Stevenson, Reducing the non-axisymmetry of a planetary dynamo and an application to Saturn. *Geophys. Astrophys. Fluid Dyn.* **21**, 113–127 (1982)
- D. Stevenson, Planetary magnetic fields. *Rep. Prog. Phys.* **46**, 555–620 (1983)
- D. Stevenson, Mercury's magnetic field: a thermoelectric dynamo? *Earth Planet. Sci. Lett.* **82**, 114–120 (1987)
- D. Stevenson, Mars' core and magnetism. *Nature* **412**, 214–219 (2001)
- D.J. Stevenson, E.E. Salpeter, The phase diagram and transport properties of hydrogen-helium fluid planets. *Astrophys. J. Suppl.* **35**, 221–237 (1977)
- F. Takahashi, M. Matsushima, Dipolar and non-dipolar dynamos in a thin shell geometry with implications for the magnetic field of Mercury. *Geophys. Res. Lett.* **33** (2006). doi:[10.1029/2006GL025792](https://doi.org/10.1029/2006GL025792)
- G. Taylor, Motion of solids in fluids when the flow is not irrotational. *Proc. R. Soc. Lond. A* **93**, 99–113 (1917)
- A. Tilgner, Zonal wind Driven by inertial modes. *Phys. Rev. Lett.* **99** (2007). doi:[10.1103/PhysRevLett.99.194501](https://doi.org/10.1103/PhysRevLett.99.194501)
- R. Vilim, S. Stanley, S. Hauck, Dynamo generation in the presence of iron snow zones: Application to mercury's weak surface field. *Eos Trans. AGU* **89**(53), Fall Meet. Suppl., Abstract U21A-0004 (2008)
- W. Watters, M. Zuber, B. Hager, Thermal perturbations caused by large impacts and consequences for mantle convection. *J. Geophys. Res.* **114** (2009). doi:[10.1029/2007JE002964](https://doi.org/10.1029/2007JE002964)
- S.A. Weinstein, The effects of a deep mantle endothermic phase change on the structure of thermal convection in silicate planets. *J. Geophys. Res.* **100**, 11719–11728 (1995)
- B. Weiss et al., Records of an ancient Martian magnetic field in ALH84001. *Earth Planet. Sci. Lett.* **201**, 449–463 (2002)
- J. Wicht et al., The origin of Mercury's internal magnetic field. *Space Sci. Rev.* **132**, 261–290 (2007)
- D. Wilhelm, S. Squyres, The Martian hemispheric dichotomy may be due to a giant impact basin. *Nature* **309**, 138–140 (1984)
- G.P. Williams, Planetary circulations: 1. Barotropic representation of Jovian and terrestrial turbulence. *J. Atmos. Sci.* **35**, 1399–1424 (1978)
- G.P. Williams, Jovian dynamics. Part III: multiple, migrating, and equatorial jets. *J. Atmos. Sci.* **60**, 1270–1296 (2003)
- J. Williams, F. Nimmo, Thermal evolution of the Martian core: Implications for an early dynamo. *Geology* **32**, 97–100 (2004)
- C. Yoder, A. Konopliv, D. Yuan, E. Standish, W. Folkner, Fluid core size of Mars from detection of the solar tide. *Science* **300**, 299–303 (2003)
- S. Zhong, M. Zuber, Degree-1 mantle convection and the crustal dichotomy on Mars. *Earth Planet. Sci. Lett.* **189**, 75–84 (2001)
- M. Zuber et al., The geophysics of Mercury: Current status and anticipated insights from the MESSENGER mission. *Space Sci. Rev.* **131**, 105–132 (2007)